Palaeogeography, Palaeoclimatology, Palaeoecology 671 (2025) 112989

Contents lists available at ScienceDirect

Palaeogeography, Palaeoclimatology, Palaeoecology

journal homepage: www.elsevier.com/locate/palaeo

Vegetation and climate record across the Carnian Pluvial episode from the Transdanubian Range, Hungary, Western Tethys

Viktória Baranyi [a], Tamás Budai [b], Viktor Karádi [c], Xin Jin [d,e,f], Wolfram M. Kürschner [g], Emőke Tóth [c,*]

[a] Department of Geology, Croatian Geological Survey (HGI-CGS), Sachsova 2, 10000 Zagreb, Croatia
[b] Department of Geology and Meteorology, University of Pécs, Ifjúság útja 6, 7624 Pécs, Hungary
[c] Department of Palaeontology, Institute of Geography and Earth Sciences, ELTE Eötvös Loránd University, Pázmány Péter sétány 1/C, 1117 Budapest, Hungary
[d] State Key Laboratory of Oil and Gas Reservoir Geology and Exploitation and Key Laboratory of Deep-time Geography and Environment Reconstruction and Applications of Ministry of Natural Resources, Chengdu University of Technology, 610059 Chengdu, China
[e] Institute of Sedimentary Geology, Chengdu University of Technology, 610059 Chengdu, China
[f] University of Trieste, Department of Mathematics, Informatics and Geosciences, 34128 Trieste, Italy
[g] Department of Geosciences and Natural History Museum, University of Oslo, Oslo, Norway

ARTICLE INFO

Editor: Howard Falcon-Lang

Keywords:
Carnian Pluvial Episode
Palynology
Paleoclimate
Palynostratigraphy
Vegetation reconstruction
Julian–Tuvalian

ABSTRACT

The Carnian Pluvial Episode (CPE) is one of the most extensively studied Triassic hyperthermal events that triggered biological turnovers both on land and in the marine realm. From a palynological perspective, the CPE is marked by a notable increase in the hygrophytic spore-pollen assemblages compared to the early Late Triassic. In the Transdanubian Range (Western Hungary), Carnian mixed clastic-carbonate successions indicate a relatively wetter climate and elevated terrestrial input into the basins during the CPE. The quantitative and qualitative palynological data from three borehole successions provided insight into the Julian and early Tuvalian vegetation history of the study area. The new palynostratigraphical data refined the age constraints of the CPE deposits spanning from the late Julian to early Tuvalian correlated to the *Duplicisporites continuus* zone from the Alpine Realm. Palynological marker taxa characteristic for the middle to late Tuvalian were absent, confirming that the well-documented hiatus between the CPE deposits and the Main Dolomite extends over large parts of the Tuvalian. A complex interplay between regional and global processes influenced the palynological assemblages that responded to both eustatic sea-level changes and climatic fluctuations. The climate change in the Julian 2 was not uniform and seemingly expressed in the palynofloras of the Transdanubian Range with a delay due to transgression, as the palynological assemblage were still predominantly characterized by xerophytic conifer pollen in the pelagic depositional site in the early CPE phase, and even they might point to highly seasonal climate at the onset of the event inferred from the proliferation of the *Enzonalasporites* group. Hygrophytic vegetation elements such as spores and cycad-bennettite pollen peaked only in the late Julian 2. Variations in the relative abundance of spores, cycad-bennettite pollen and marine palynomorphs showed the combined effects of local sea-level changes and humid climatic episodes in controlling terrestrial influx from the latest Julian 2–Tuvalian onwards. The palynofloras point to aridification from later in the early Tuvalian, indicating the waning of the pluvial phase.

1. Introduction

The generally arid Late Triassic climate regime (e.g., Preto et al., 2010) was punctuated by a geologically abrupt episode of pronounced climate change and carbon cycle perturbation labelled as the Carnian Pluvial Episode or CPE, which occurred at *ca.* 234–232 Ma with a duration of ~1 myr or more (Simms and Ruffell, 1989, 1990; Kozur and Bachmann, 2010; Sun et al., 2016; Miller et al., 2017; Dal Corso et al., 2020; Lu et al., 2021). The CPE can be characterized as a Mesozoic hyperthermal event with a primarily warming phase (Trotter et al., 2015), multiple negative carbon isotope excursions (NCIEs) recorded in marine as well as in terrestrial sedimentary archives (e.g., Dal Corso

* Corresponding author.
E-mail addresses: vbaranyi@hgi-cgs.hr (V. Baranyi), emoke.mohr@ttk.elte.hu (E. Tóth).

https://doi.org/10.1016/j.palaeo.2025.112989
Received 6 January 2025; Received in revised form 29 April 2025; Accepted 29 April 2025
Available online 1 May 2025

et al., 2012, 2015, 2018; Miller et al., 2017; Jin et al., 2020, 2022), enhanced hydrological cycling (Rostási et al., 2011; Ruffell et al., 2016; Barrenechea et al., 2018; Pecorari et al., 2023) and a shift to more humid conditions (e.g., Ogg, 2015; Ruffell et al., 2018; Simms and Ruffell, 2018). The CPE is commonly linked to the eruption of the Wrangellia Large Igneous Province based on the coincidence of peaks of Hg concentrations and NCIEs (Furin et al., 2006; Dal Corso et al., 2012; Mazaheri-Johari et al., 2021; Jin et al., 2023; Zhang et al., 2024). The carbon cycle perturbation resulting from greenhouse-gas emissions affected the entire Earth-ocean-atmosphere system, thereby intensifying the Pangean megamonsoon circulation (Parrish, 1993; Hu et al., 2023). To date, four negative carbon isotope excursions (NCIEs) have been identified and correlated across the Western Tethys realm (Dal Corso et al., 2015, 2018) with the first, sharp NCIE at the Julian 1–2 boundary marking the onset of the event (Fig. 1A). The carbon cycle and climatic perturbation associated with the CPE lasted at least until the mid Tuvalian in the Western Tethys with the last NCIE placed at the boundary of the Tuvalian 1 and 2 at the boundary between the *Tropites dilleri* and *T. subbulatus* zones (Dal Corso et al., 2018, 2020). The elevated greenhouse gas emissions caused a prominent shift to a more humid and warmer climate and accelerated the hydrological cycle that resulted in an increase in terrestrial runoff and siliciclastic input into the ocean (e.g., Rostási et al., 2011; Pecorari et al., 2023), which in turn led to the crisis of the carbonate factories in shallow seas (Fig. 1A, see e.g., Hornung et al., 2007; Rigo et al., 2007; Jin et al., 2020). Additionally, high extinction rates were observed among marine invertebrates (ammonites, bryozoans, crinoids) and conodonts (Simms and Ruffell, 1989, 2018; Dal Corso et al., 2020). The global impact of the climate change resulted in the expansion of the wet climate belt and an increase in the abundance of hygrophytic vegetation elements accompanied by the widespread return of coal seams following the significant coal gap after the End-Permian extinction event (e.g., Retallack et al., 1996; Roghi, 2004; Hochuli and Frank, 2000; Roghi et al., 2010, 2022; Mueller et al., 2016a, 2016b; Baranyi et al., 2019a, 2019b; Mancuso et al., 2020; Fijałkowska-Mader et al., 2021; Lu et al., 2021; Li et al., 2022; Peng et al., 2022; Zhang et al., 2023). Furthermore, climate change across the CPE likely initiated the diversification of dinosaurs (Bernardi et al., 2018; Mancuso et al., 2020), and marked a turning point in the evolution of several plant groups e.g., Bennettitales, Podocarpaceae, Pinaceae, and Cheirolepidiaceae conifers that subsequently became important components in younger Mesozoic or modern floras, while “older” Mesozoic conifer families (e.g., Majonicaceae, Voltziaceae) declined in the aftermath of the event (Kustatscher et al., 2018; Dal Corso et al., 2020). An unusual aspect of the CPE is the first major occurrence of fossil amber (Gianolla et al., 1998b; Csillag and Földvári, 2005; Roghi et al., 2006; Seyfullah et al., 2018a, 2018b; Forte et al., 2022) that suggests widespread terrestrial ecosystem stress including a wide array of physical damage from extreme weather events such as storms or wildfires, as well as the effects of climate change that led to an increase in resin production by conifers (Seyfullah et al., 2018a, 2018b; Forte et al., 2022).

Palynological data are widely applied as environmental proxies (e.g., Birks et al., 2016). Fossil spore and pollen assemblages played a pivotal role from early on in the CPE research, enabling the detection of vegetation and climatic patterns (e.g., Visscher et al., 1994; Roghi, 2004). Previous palynological studies have corroborated the humid climatic shift and an increase in the abundance of hygrophytic vegetation elements across the Western Tethys (Planderová, 1980; Blendinger, 1988; Roghi, 2004; Roghi et al., 2010; Mueller et al., 2016b; Baranyi et al., 2019b; Mazaheri-Johari et al., 2021) and Eastern Tethys (Lu et al., 2021; Li et al., 2022; Peng et al., 2022; Zhang et al., 2023), Central European Basin (Visscher et al., 1994; Fijałkowska-Mader et al., 2021), Western Europe (UK, Baranyi et al., 2019a), and the Boreal Realm (Mueller et al., 2016a). In the Alpine region, the distinct clastic pulses during the CPE were associated with unique palynological assemblages (Roghi et al., 2010), thus the palynological changes could be interpreted as having climatic as well as biostratigraphical significance. Yet the climatic interpretation of a clear humid shift during the CPE should be viewed with caution, as the wet phases may not have been prevalent, and/or homogeneously distributed in time and space (e.g., Lindström et al., 2017; Baranyi et al., 2019a). Nevertheless, many geochemical and palaeontological studies (including palynological research) concentrate only on the initial stages of the event with comparatively less work dedicated to the subsequent phase of the CPE or the recovery period in the Tuvalian.

In the Transdanubian Range (Western Hungary) numerous outcrops and boreholes document Carnian marine successions (Figs. 1B–E) with continuous stratigraphical record (e.g., Budai and Haas, 1997; Budai et al., 1999; Nagy and Csillag, 2002; Haas et al., 2012; Dal Corso et al., 2015, 2018) that enables the temporally and spatially comprehensive investigation of palynological assemblages throughout the entire Julian 2 and early Tuvalian. Palynological data across the CPE from Hungary were represented mainly by semi-quantitative or presence-absence data (Góczán et al., 1983; Góczán et al., 1991a; Góczán and Oravecz-Scheffer, 1996a, 1996b) or concentrated on the onset of the event (Baranyi et al., 2019b). The objective of this study is to provide a comprehensive view on vegetation and climatic changes in the Transdanubian Range during the Carnian Pluvial Episode. The quantitative and qualitative palynological dataset from three borehole successions – among them two profiles that have not been studied in detail before – representing late Julian 2 and early Tuvalian, demonstrate the extent to which palynofloras were influenced by global climatic changes and local environmental factors.

2. Geological setting

2.1. Geological and facies evolution of the Transdanubian Range in the Triassic

The Transdanubian Range unit, now situated in the NW part of the Carpathian-Pannonian Basin (Figs. 1C–D) was part of the passive margin of the Western Tethys during the Triassic (Figs. 1B–C), wedged between the East Alpine and the Southern Alpine tectonic units (Haas et al., 1995; Csontos and Vörös, 2004). The Balaton Highland forms the southeastern flank of the SW–NE oriented Alpine compressional syncline structure of the Transdanubian Range, made up predominantly of Triassic formations with a total thickness of about 3 km (Figs. 1D–E).

The Late Permian–Early Triassic facies evolution is characterized by marine transgression and the flooding of the alluvial plains and coastal lagoons, which resulted in the formation of a shallow mixed siliciclastic-carbonate ramp (e.g., Haas and Budai, 1995; Haas et al., 2012). In the middle Anisian, the extensional tectonic movements in the western end of the eastward-progressing Tethys resulted in the differentiation of the former (early Anisian) carbonate ramp leading to the development of horst and graben-style paleotopography with deeper hemipelagic basins divided by isolated carbonate platforms until the early Carnian (e.g., Budai and Vörös, 1993, 2006). In the larger area of the Balaton Highland, the lowermost Carnian (Julian 1, previously Cordevolian) sequence is characterized by the hemipelagic Füred Limestone Formation (Fig. 1E) comprising micritic limestone layers with thin marl intercalations in its uppermost segment (Budai and Haas, 1997; Budai et al., 1999). Carbonate sedimentation in the deeper hemipelagic settings was interrupted by the arrival of a significant influx of terrestrial siliciclastic material from the Julian 1–Julian 2 boundary onwards, represented by the mixed carbonate-clastic packages of the Veszprém Marl Formation (Fig. 1E) that reached a total thickness of 600 m in the hemipelagic basins (e.g., Budai et al., 1999; Haas and Budai, 1999; Haas et al., 2012) (Figs. 1E, 2). The onset of the CPE marked by the first NCIE coincided with this lithological transition in the Balaton Highland (Dal Corso et al., 2015, 2018). However, the sedimentation of the marl packages was not continuous due to episodes of highstand progradation of the adjacent carbonate platforms, which led to the deposition of pelagic carbonates (Nosztor Limestone Member), toe-of-slope sediments

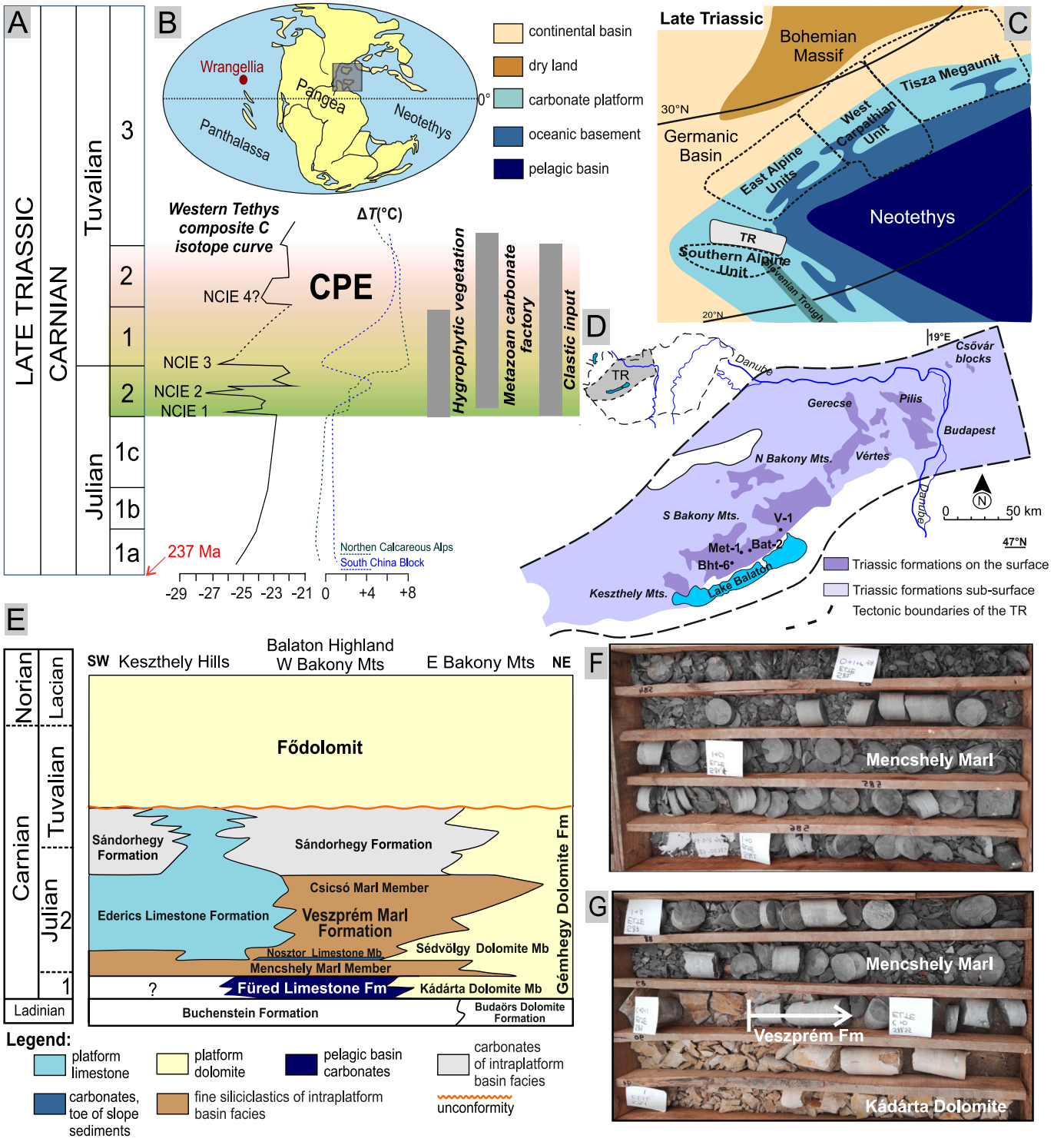

Fig. 1. Carbon cycle and environmental perturbation during the Carnian Pluvial Episode (CPE) together with the geological setting of the study area in the Western Tethys. A. Composite carbon isotope curve and key environmental changes in the Western Tethys during the CPE after Dal Corso et al. (2015, 2018, 2020). Conodont paleotemperature data from Rigo and Joachimski (2010), Trotter et al. (2015), and Sun et al. (2016). B-C. Paleogeographical setting of the Transdanubian Range in the western part of the Tethys Ocean during the Late Triassic (Haas et al., 1995). D. Geological setting of the Transdanubian Range showing Triassic formations on the surface with the location of the studied boreholes (modified after Haas et al., 2010). E. Ladinian to Late Triassic lithostratigraphic scheme of the Transdanubian Range (modified after Haas and Budai, 2014). F–G. Impression of the lithological composition of the Veszprém Formation at the onset of the CPE. F. Interval between ~582–587 m of the Veszprém V-1 borehole showing the grey clayey marls of the Mencsehely Marl Member. G. Interval between ~587–592 m of the Veszprém V-1 borehole at the Szépvizér core repository of the Hungarian Geological Survey showing the Kádárta Dolomite Member overlain by the clayey marl deposits of the Mencshely Marl Member.

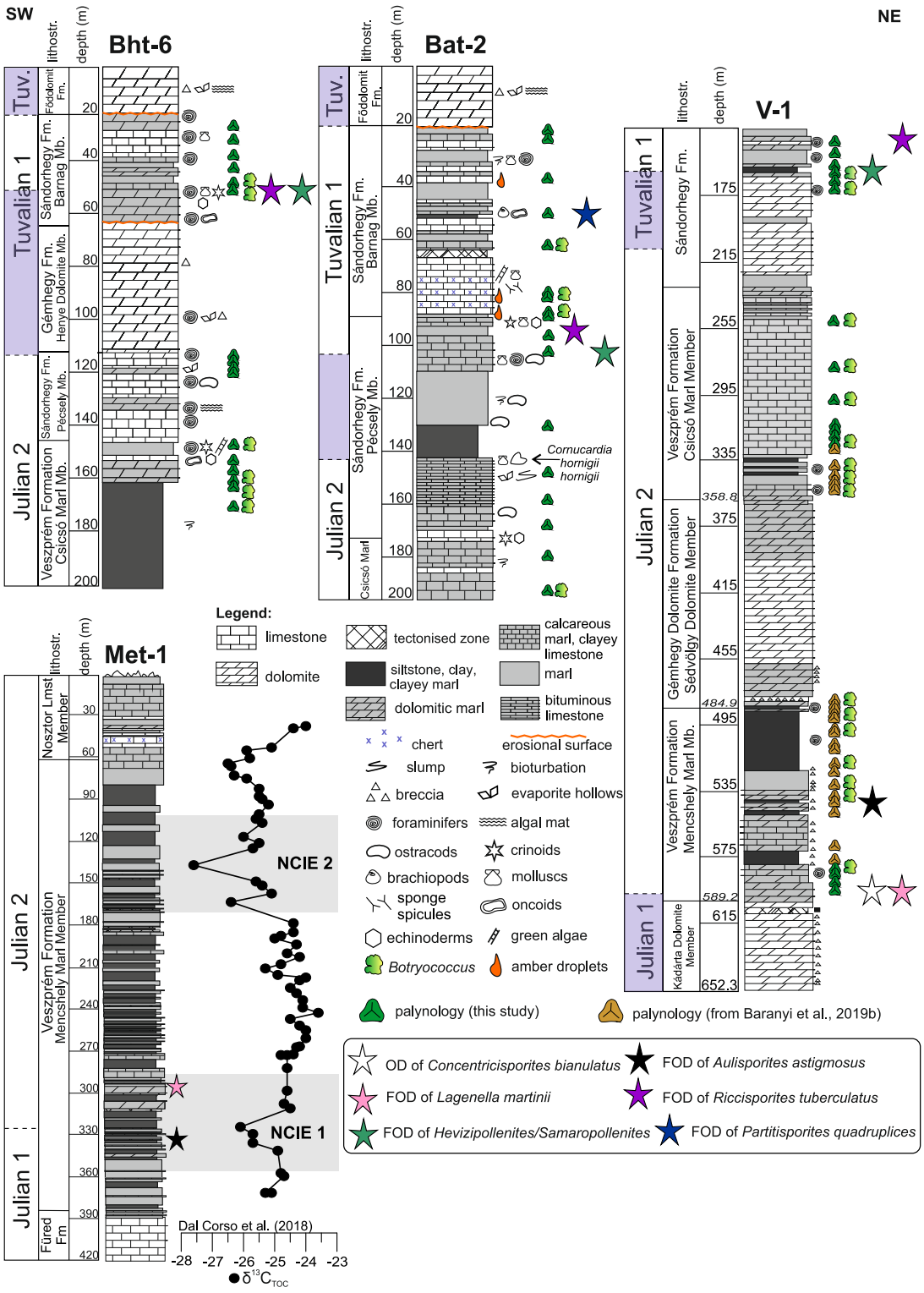

Fig. 2. Lithostratigraphic log of the studied borehole successions with the indication of the sampled horizons for palynological analysis. Biostratigraphically significant palyno-events and local first occurrences are also indicated. Lithostratigraphic logs and biostratigraphic constraints are from Góczán and Oravecz-Scheffer (1996a, 1996b), Nagy and Csillag (2002), Rostási et al. (2011), Baranyi et al. (2019b), and Tóth et al. (2024). Purple shaded areas represent intervals of uncertain age assignment. The Mencshely Met-1 borehole section is also illustrated besides the newly studied successions in order to show the available chemostratigraphical information from the Veszprém Formation (C-isotope curve after Dal Corso et al., 2018). (For interpretation of the references to colour in this figure legend, the reader is referred to the web version of this article.)

or intercalated platform carbonates dividing the marls into a lithologically very similar lower (Mencshely Marl Member) and upper (Csicsó Marl Member) marl unit (Figs. 1E, 2).

The clastic influence together with lime mud originating from the neighbouring shallow-water areas during the Julian 2 filled up the intraplatform basins. This led to the establishment of a shallow ramp environment with great variety of lithologies and facies types depending on the proximity to adjacent carbonate platforms, emerged land, presence of restricted basins, and amount of terrestrial influx represented by the Sándorhegy Formation (Fig. 1E). As a consequence of the inherited dissected bottom topography and the filling of the basins, coupled with a late Julian sea-level fall (Nagy, 1999; Jin et al., 2022; Pecorari et al., 2023), some parts of the shallow basins became separated with restricted circulation resulting in water column stratification represented by the lower part of the Pécsely Member (Nagy, 1999; Nagy and Csillag, 2002). In the stagnant water column, anoxic-dysoxic conditions prevailed, resulting in the deposition of organic-rich bituminous limestone laminae with occasional subtidal microbial mats while pseudomorhps after dissolved gypsum in intercalating dolomite beds infer hypersaline bottom waters (Nagy, 1999) (Fig. 2). A subsequent sea level rise opened the basins marked by the deposition of bioclastic and cherty limestones (Fig. 2, Budai and Haas, 1997; Haas and Budai, 1999; Nagy, 1999; Nagy and Csillag, 2002). Episodic increases of terrigenous input temporally diminished the activity of carbonate factories, as evidenced by the alternation of marl and clayey limestone-limestone in the Barnag Member which represents the upper part of the Sándorhegy Formation (Fig. 2), which is assigned to the Barnag Member (Nagy, 1999; Nagy and Csillag, 2002). The infill of the intra-platform basins during the late Julian 2 and early Tuvalian apparently levelled the topography enabling the deposition of the peritidal Fődolomit Formation (equivalent of the Main Dolomite/Hauptdolomit/Dolomia Principale) after a stratigraphical gap and denudation of the upper part of the sequence. Detailed lithological and facies descriptions for each studied borehole succession (Fig. 2) is provided in the Supplementary material.

2.2. Biostratigraphical age constraints and correlation

The late Julian–Tuvalian successions of the Balaton Highland are largely devoid of any stratigraphically robust index fossils due to the scarcity of ammonoid and conodont faunas in the mixed carbonate-clastic sediments associated with the CPE. Some of the studied units have biostratigraphic anchors from other locations within the Transdanubian Range (e.g., Dosztály et al., 1989; Budai et al., 1999) but they provide only indirect age constraints as none of them have been recovered from the studied borehole successions. Ammonoid marker of the Füred Limestone (*Trachyceras aon*) indicates lower Julian 1 ("Cordevolian") age, while other scarce ammonite findings (*Neoprotrachyceras* sp. and *Sirenites* sp.) from the same formation (Budai et al., 1999) are highly questionable and should be reviewed (personal communication with Leopold Krystyn 2024). Consequently, there is some uncertainty in the biostratigraphical age assignment of the transition between the Füred and Veszprém Formation and the Mencsehely Marl Member. Index taxa of the Nosztor Limestone Member (*Austrotrachyceras austriacum*) and ammonoids of the Csicsó Marl (*Neoprotrachyceras baconicum*) from the Csukrét Ravine suggest Julian 2 age for the middle and upper part of the Veszprém Formation (Budai et al., 1999; Dal Corso et al., 2015; Tóth et al., 2024).

The bivalve *Cornucardia hornigii hornigii*, which was found in large numbers in the thick-bedded limestones overlying the bituminous limestone unit of the Sándorhegy Formation all over the Balaton Highland (Fig. 2), is indicative of the Tuvalian substage (Végh-Neubrandt, 1982). In the Barnag Bat-2 borehole its presence is documented at ~141–142 m (Nagy and Csillag, 2002). This bivalve is found very frequently together with *Neomegalodon carinthiacus* in a thick-bedded limestone bed in the lowermost part of the Barnag Member in the Nosztor Valley outcrop of the Sándorhegy Formation (Budai et al., 1999; Nagy, 1999). In the Alpine region, mass occurrences of *Cornucardia hornigii* are always found overlying typical Julian fossil assemblages in the Carnian strata indicating a Tuvalian age (Zapfe, 1972). Based on foraminifer distributions in particular the first occurrences of *Aulotortus sinuosus, Nodosaria raibliana, Triadodiscus eomesozoicus*, the Julian–Tuvalian boundary was placed at 91–90 m in the Barnag Bat-2 and at 116.5 m in the Balatonhenye Bht-6 cores in the upper part of the Pécsely Member (Góczán and Oravecz-Scheffer, 1996a, 1996b). However, these species seem to be present already from the Ladinian and only becoming more common in the Late Triassic (e.g., Gale, 2012; Ueno et al., 2018) likely connected to facies change. In the Veszprém V-1 core, the boundary was placed at 205.0 m but only following facies analogies from other successions (Góczán and Oravecz-Scheffer, 1996a, 1996b).

Based on the available biostratigraphical data and facies correlation to the Alpine Carnian sections (e.g., Budai et al., 1999; Dal Corso et al., 2018), the Füred Limestone in the Transdanubian Range (Julian 1) is coeval with the upper part of the San Cassiano Formation in the Dolomites, the Predil Limestone of the Julian Alps, and the upper part of the Reifling Formation in the Northern Calcareous Alps (NCA). The Veszprém and Sándorhegy Formation can be correlated with the Heiligkreuz Formation. The Julian–Tuvalian boundary can be placed in the uppermost Dibona Member of the Heilgkreuz Formation in the Dolomites (Dal Corso et al., 2018), and in the lower–middle part of the Sándorhegy Formation in the Transdanubian Range (Góczán and Oravecz-Scheffer, 1996a, 1996b). The upper part of the Barnag Member is based on its lithological features and stratigraphical superposition, very similar to the upper part of the Heiligkreuz Formation, the Lagazuoi Member. This unit may represent a possibly heteropic facies of the terrigenous Raibl Formation (Raibl Beds/Raiblerschichten) which is absent from the studied sequences in the Transdanubian Range (Budai et al., 1999). Furthermore, both the Sándorhegy and Heiligkreuz formations are capped by a pronounced emersion horizon with breccias and signs of karstification (Budai et al., 1999; Breda et al., 2009) The lithology and facies of the Sándorhegy Formation bears some resemblance to certain parts of the Opponitz Formation in the Lunz area, Northern Calcareous Alps (NCA) and the Tor Beds (Formation) in the Julian Alps (Budai et al., 1999).

3. Material and methods

All core samples were obtained from the Szépvizér core repository of the Hungarian Geological Survey (currently part of the Supervisory Authority for Regulatory Affairs). Quantitative palynological analyses have been carried out on 51 selected samples from three borehole successions (Supplementary Material Tables S1–S3). Eighteen samples from Veszprém V-1 (46°58′44.61" N, 17°46'21.23" E), 17 samples from Barnag Bat-2 (46°58′44.61" N, 17°46′21.23″ E), and 16 samples from the Balatonhenye Bht-6 (46°55′20.23" N, 17°37'35.11" E) extending the dataset from Baranyi et al. (2019b). In addition to the previously sampled intervals, three new intervals have been selected from the Veszprém V-1 borehole (588.35–580 m, 252–330 m, and 141–164.5 m) for palynological analysis (Fig. S1, Supplementary material Table S1). There was no palynological sampling in Bht-6 between 117 and 51 m as the lithology in this interval is primarily composed of dolomite. In the VeszprémV-1 borehole no coring took place in the upper part of the Veszprém Formation and large parts of the Sándorhegy Formation, therefore only the interval between 141 and 164.5 m was available for sampling from the upper part of the core.

Palynological sample preparation followed the protocol of Moore et al. (1991) including soaking of approximately 15–20 g of crushed sediment in sodium-pyrophosphate ($Na_4P_2O_7$) for 24 h in order to disintegrate clay minerals followed by acid treatment with 10 % HCl and 40 % HF to dissolve the carbonate and silicate fraction respectively. At the beginning of the acid treatment, one tablet containing the exotic marker *Lycopodium* was added to each sample (one tablet contains

13,761 *Lyocopodium clavatum* spores). The HF step was performed in hot water bath at 60 °C by cooking the samples in the acid for 90 min, twice repeated if the disintegration of the silicates was inadequate. Following the final HF treatment, the residue was cooked in concentrated HCl for 90 min to dissolve any residual fluoride minerals. Heavy liquid separation was performed with $ZnCl_2$ (specific gravity 2.1 kg/l) in order to separate any additional mineral fractions and the organic residue. After washing to neutrality, the organic residue was sieved with a 10 μm mesh-size sieve and mounted in glycerine jelly on glass slides. The microscopy slides were analysed with an Olympus BH2 RFC trinocular transmitted light microscope at magnifications of ×200, ×400. The photomicrographs were captured using an AmScopeTM camera adapter and AmScope v.3.7 software. Abundance diagrams were plotted with TiliaGraph (Grimm, 1987) based on counting about 300 palynomorphs per sample or counting two entire slides in instances where the total palynomorph abundance was low. The classification of the palynomorphs is based on the works of Klaus (1960), Schulz (1967), Praehauser-Enzenberg (1970), Orłowska-Zwolińska (1983), Van der Eem (1983), Góczán and Oravecz-Scheffer (1996a), Roghi (2004), and Fijałkowska-Mader et al. (2015). A list of all identified taxa with full author citation below generic level and the original counts for dispersed spore-pollen taxa, and marine palynomorphs are given in the Supplementary material tables S1–S3).

The paleoenvironmental interpretation of the palynomorph assemblages is based on the known or presumed botanical and ecological affinity of the dispersed sporomorphs' parent plants (Supplementary material tables S4–S5). Spores and pollen were classified as hygrophytic, xerophytic or intermediate in accordance with the concept proposed by Visscher and Van der Zwan (1981). Intermediate groups were defined based on the works of Wang et al. (2005) and Li et al. (2020, 2022). The hygrophyte to xerophyte ratio (H/X) is a close resemblance to the spore to pollen ratio, unless any exceptions are noted in the ecological affinity of the taxa (Supplementary material table S4). The intermediate to xerophyte ratio (I/H) gives an estimation of the relationship between seed fern, cycad-bennettite pollen, and coastal conifer to upland conifer taxa. For a more comprehensive view on the changes in the palynological assemblages, Sporomorph Ecogroup Model (SEG) and environmental proxy data from the adjacent Mencshely Met-1 core (Baranyi et al., 2019b) were partly re-interpreted (Supplementary material table S5) in order to compare the onset of the CPE from a basinal profile to the periplatform V-1 succession.

The Sporomorph Ecogroup Model (SEG) method (Abbink et al., 2004; Kustatscher et al., 2012; Li et al., 2020, 2022) was applied to distinguish between different plant communities. The SEG model is used to identify habitats and co-existing communities and to interpret them in a paleoenvironmental context, i.e., sea level and climatic changes. The upland or hinterland SEG represents plant communities that inhabit well drained higher terrain, well above groundwater level, and at considerable distance from watercourses. The coastal SEG includes communities found on the coastal plain, or along the coastline, in areas not submerged by the sea, but affected by salt spray. The river SEG reflects riverbank communities that are periodically submerged, the dry lowland SEG reflects floodplain vegetation that are episodically submerged. The wet lowland SEG represents marshes and swamps. As pollen producers for the *Alisporites* group can be both upland and lowland communities produced by conifers and/or seed ferns (e.g., Abbink et al., 2004; Paterson et al., 2016), this group was plotted separately from the other ecogroups following as described in Baranyi et al. (2024). Alete bisaccate pollen grains like *Alisporites* spp. were assigned to the upland SEG (Abbink et al., 2004; Paterson et al., 2016) with the exception of *A. thomasii* and *Vitreisporites pallidus*. The marine SEG represents fully marine associations with marine palynomorphs including acritarchs, foraminiferal test linings, and scolecodonts. The brackish-freshwater SEG with prasinophytes and *Botryococcus* includes freshwater and proximal associations that can indicate salinity variations and freshwater influence.

4. Results

4.1. Palynological assemblages

The studied successions reveal diverse and abundant palynological assemblages with 102 identified taxa including 43 spore, 59 pollen taxa, and eight aquatic palynomorphs including acritarchs (*Micrhystridium breve* Fig. 5 AB, *M. pentagonale* Fig. 3D, *Verychachium* sp. Figs. 3B–C, and *Leiofusa* sp.), prasinophytes (*Dictyotidium reticulatum* Fig. 3E, *D. tenuiornatum*), scolecodonts (Fig. 3A), and freshwater organisms such as green algae *Botryococcus braunii* (Fig. 5 AG) and *Brodispora striata* also known as *Circulisporites* or *Concentricystis* (Figs. 3–8). The wall colour varies between pale yellow to golden brown-brown, their SCI index ranges from 2 to 7 depending on wall-thickness variations and ornamentation between taxa (Batten, 2002). The preservation of palynomorphs is generally good to moderate in the Veszprém Formation, with a moderate to rather poor palynomorph preservation in the Sándorhegy Formation, particularly in core Barnag Bat-2 where many grains are partly mineralized, and frequent pyrite overgrowth hampers the identification of many spores and pollen grains. The representative palynomorphs are illustrated in Figs. 3–6.

The palynological spectrum is primarily composed of terrestrial palynomorphs but marine taxa, particularly foraminiferal test linings and acritarchs, attain high relative abundances in several intervals (Figs. 7–8). Stratigraphically constrained cluster analysis in *Tilia* (Grimm, 1987) distinguishes three informal local assemblages in the Veszprém V-1 core (Fig. 7). The *singhii-acutus-vigens* local assemblages (V-1541–588.35 m, Fig. 7) has already been identified by Baranyi et al. (2019b) and is characterized by the common occurrence of alete bisaccate pollen (*Alisporites aequalis* Figs. 3H, *A. giganteus* Fig. 4A, *A. parvus, A. robustus* Fig. 4D, up to ~5–10 % in total), taeniate (striate) pollen (e.g., *Lunatisporites acutus* Figs. 4F, 6I, *Lueckisporites singhii* Fig. 3I, *Striatoabietites aytugii* Fig. 3L, and *Infernopollenites sulcatus* Fig. 3G, ~20 % in total), Circumpolles pollen (Figs. 3O–R, 5–15 %) and monosaccate pollen e.g., *Enzonalasporites vigens* (Figs. 3K, N, 4M, P) or *Vallasporites ignacii* (each ~20 %). Spore taxa constitute only a minor component of the Mencshely Marl palynological assemblages, with a relative abundance usually below <5 %. Aquatic palynomorphs are very frequent in the lowermost part exceeding 90 % of the palynomorphs at 587 m.

The overlying *acutus-vigens*-Circumpolles (V-1 493–538 m, Fig. 7) assemblage differs from the *singhii-acutus-vigens* assemblage by the higher relative abundance of Circumpolles pollen (up to 30 %) represented by e.g., *Duplicisporites granulatus* (Fig. 3P), *D. continuus* (Figs. 3R, 4R), *Camerosporites secatus* (Figs. 3Q, 4Q), *Partitisporites maljawkinae* (Figs. 3O, 6AA), *P. novimundanus*, *P. tenebrosus* (Fig. 6R, X), and *Praecirculina granifer* (Fig. 6V). Spores become more frequent in the assemblage forming up to 15 % of the total palynomorph sum represented by laevigate trilete spores (*Calamospora tener* Fig. 5F, *Deltoidospora mesozoica, Todisporites* spp., and *Dictyophyllidites harrisii*) and *Aratrisporites* spp. while the relative abundance of marine palynomorphs shows a decreasing trend. The interval between 335 and 492 m was not assigned to any local zones as it shows transitional character towards the under- and overlying assemblages. Moreover, this interval is also interrupted by the dolomites of the Sédvölgy Member (see Figs. 2 and 7).

Palynological assemblages of the Csicsó Marl Member in the Veszprém V-1 core (252–330 m, Fig. 7) are assigned to the local *Aratrisporites-astigmosus-densus* assemblage already identified in Baranyi et al. (2019b) and characterized by a significant increase in spore proportions (up to ~35 %), *Aulisporites astigmosus* (Figs. 5 CE–AE, up to 5 %), and *Cycadopites* spp. (e.g., *C. carpenteri* Fig. 5AA, *C. potonieii* Fig. 5 AC, up to 15 %). The most common spore taxa are *Aratrisporites* spp., (*A. scabratus, A. palettae* Figs. 5A–B), *Calamospora tener* (Fig. 5F), and laevigate trilete spores (*Deltoidospora mesozoica, Dictyophyllidites harrissii* Fig. 5Q, *Todisporites* spp., *Concavisporites crassexinus* Fig. 5P, and *Paraconcavisporites lunzensis* Fig. 5R). Other characteristic taxa include: *Camarozonosporites rudis* (Fig. 5U), *Gibeosporites lativerrucosus* (Fig. 5I),

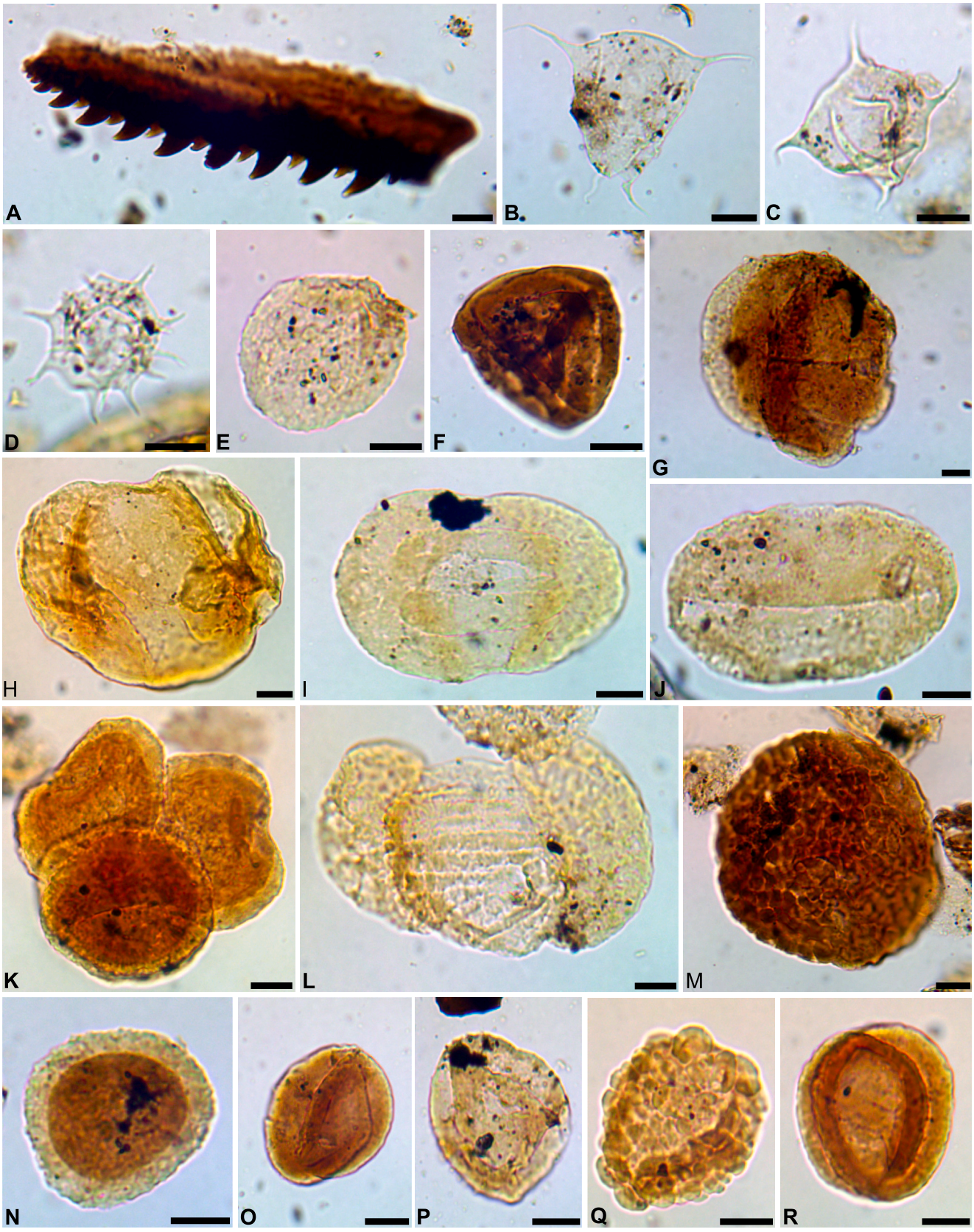

Fig. 3. Selected palynomorphs from the lowermost part of the Veszprém Formation, Veszprém V-1 borehole from 580.0 to 588.35 m. The scale bar represents 10 μm for all figures. A. Scolecodont 588.35 m. B. *Verychachium* sp. 588.35 m. C. *Verychachium* sp. 588.35 m. D. *Micrhystridium pentagonale* 588.35 m. E. *Dictyotidium reticulatum* 584.0 m. F. cf. *Concentricisporites bianulatus* 588.35 m. G. *Infernopollenites sulcatus* 584.0 m. H. *Alisporites aequalis* 582.0 m. I. *Lueckisporites singhii* 580.0 m. J. *Ovalipollis ovalis* 588.35 m. K. *Enzonalasporites vigens* triad 582.0 m. L. *Striatoabietites aytugii* 580.0 m. M. *Verrucosisporites morulae* 584.0 m. N. *Enzonalasporites vigens* 580.0 m. O. *Partitisporites maljawkinae* 588.35 m. P. *Duplicisporites granulatus* 588.35 m. Q. *Camerosporites secatus* 582.0 m. R. *Duplicisporites continuus* 582.0 m.

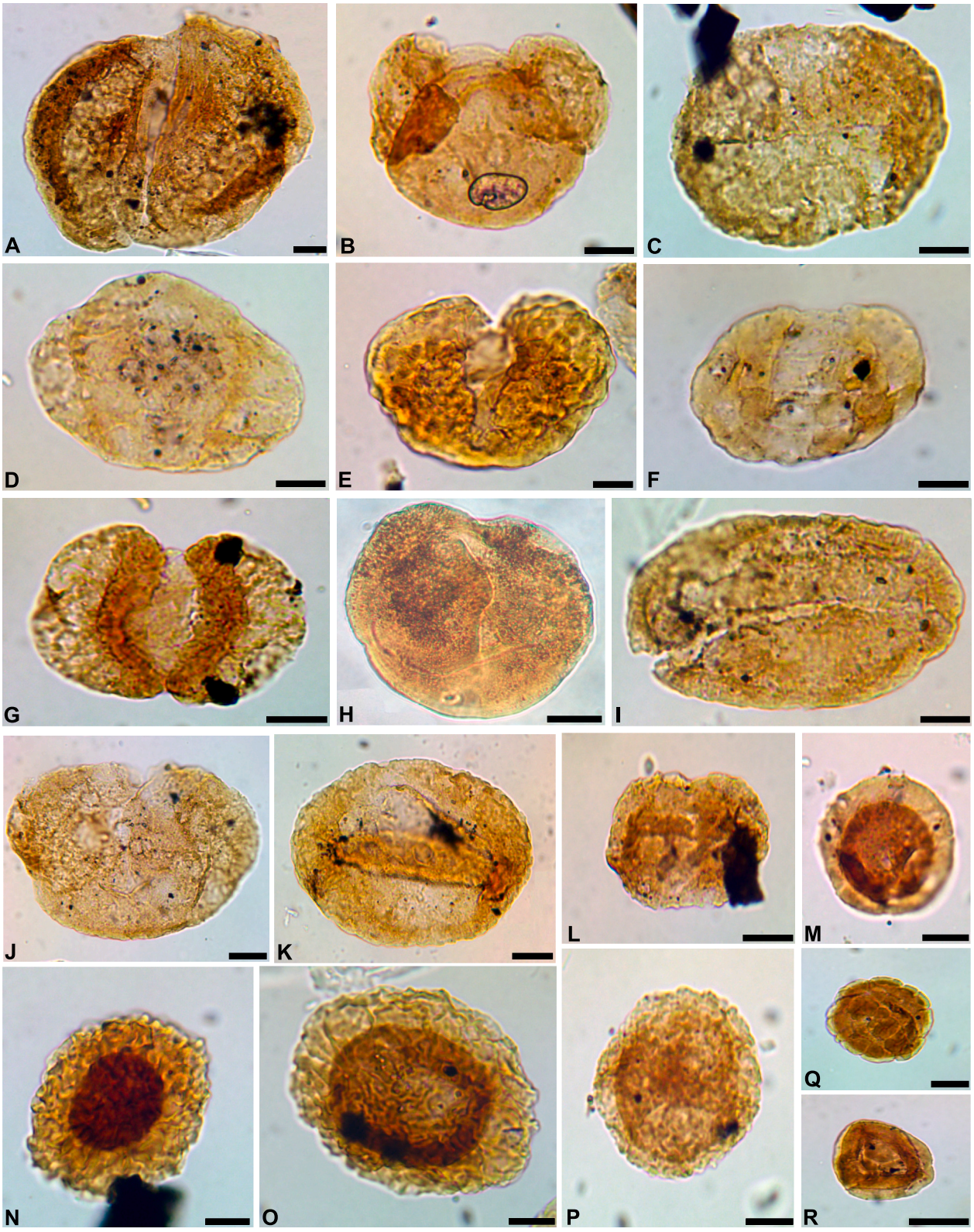

Fig. 4. Selected bisaccate, monosaccate, and Circumpolles pollen from the Csicsó Marl Member of the Veszprém Formation from 252.0 to 334.6 m in the Veszprém V-1 borehole. The scale bar represents 10 μm for all figures. A. *Alisporites giganteus* 276–278 m. B. *Pityosporites devolvens* 276–278 m. C. *Ovalipollis ovalis* 326.0 m. D. *Alisporites robustus* 297–300 m. E. *Pityosporites devolvens* 328.0 m. F. *Lunatisporites acutus* 276–278 m. G. *Platysaccus queenslandi* 276–278 m. H. *Staurosaccites quadrifidus* 334.6 m. I. *Ovalipollis lunzensis* 276–278 m. J. *Rimaesporites potoniei* 276–278 m. K. *Staurosaccites quadrifidus* 328.0 m. L. *Ovalipollis minimus* 328.0 m. M. *Enzonalasporites vigens* 252.0 m. N. *Patinasporites explanatus* 317.0 m. O. *Patinasporites densus* 326.0 m. P. *Enzonalasporites vigens* 276–278 m. Q. *Camerosporites secatus* 326.0 m. R. *Duplicisporites continuus* 276–278 m.

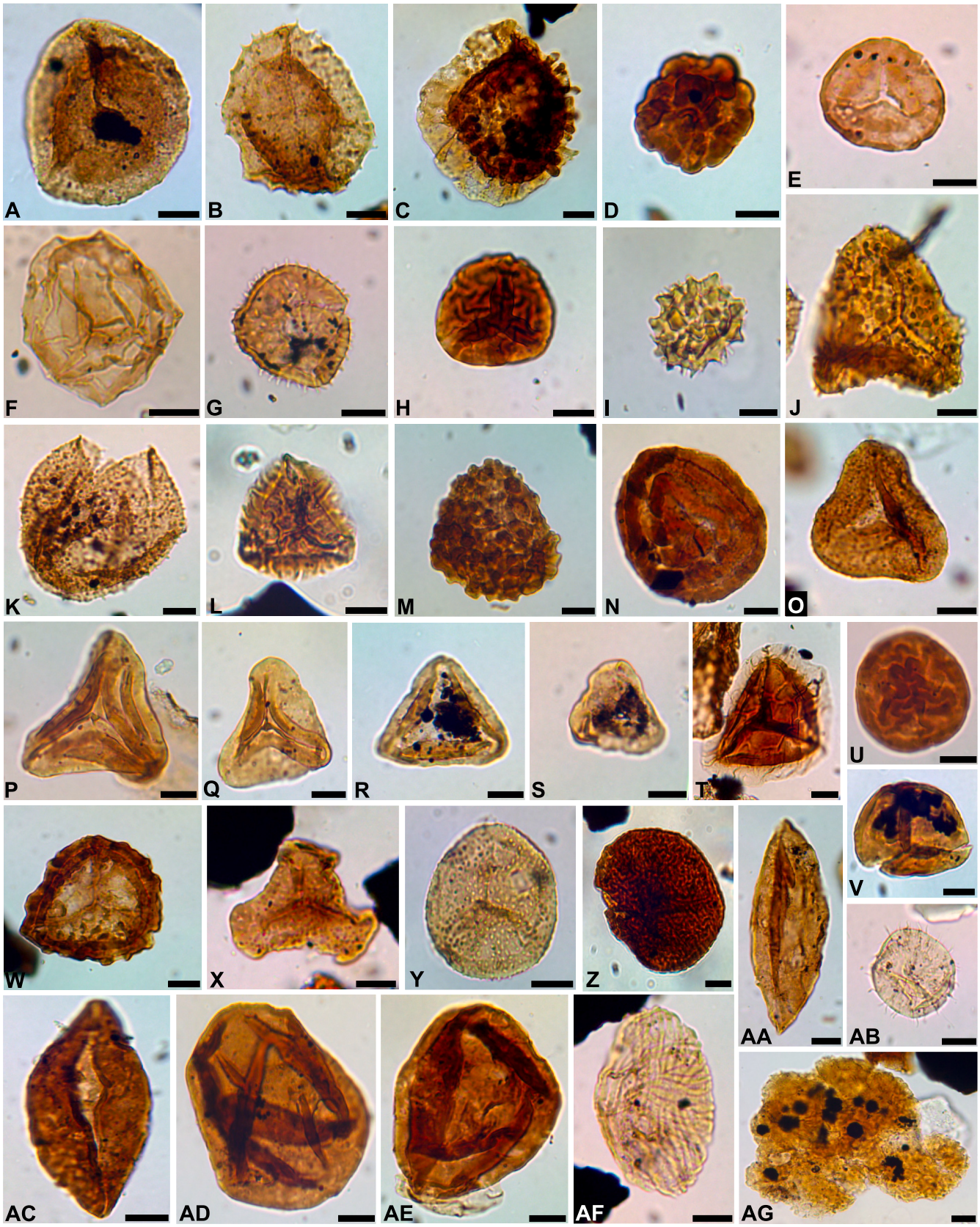

(caption on next page)

Fig. 5. Selected spore-pollen and marine palynomorphs from the Veszprém and Sándorhegy formations from the Veszprém V-1, Barnag Bat-2, and Balatonhenye Bht-6 cores. The scale bar represents 10 μm for all figures. A. *Aratrisporites scabratus* V-1 330.0 m. B. *Aratrisporites palettae* V-1 326.0 m. C. *Kraeuselisporites cooksonae* V-1 326.0 m. D. *Uvaesporites gadensis* V-1 326.0 m. E. *Rogalskaisporites cicatricosus* V-1 159–160 m. F. *Calamospora tener* V-1 328.0 m. G. *Anapiculatisporites telephorus* V-1 328.0 m. H. *Lycopodiacidites kuepperi* V-1 328.0 m. I. *Gibeosporites lativerrucosus* V-1 159–160 m. J. *Neoraistrickia taylorii* V-1 276–278 m. K. *Porcellispora longdonensis* V-1 276–278 m. L. *Zebrasporites kahleri* Bht-6 160.4 m. M. *Trilites tuberculiformis* V-1 326.0 m. N. *Striatella seebergensis* V-1 297–300 m. O. *Conbaculatisporites mesozoicus* V-1 276–278 m. P. *Concavisporites crassexinus* V-1 328.0 m. Q. *Dictyophyllidites harrissii* V-1 276–278 m. R. *Paraconcavisporites lunzensis* V-1 326.0 m. S. Dwarfed trilete spore V-1 328.0 m. T. *Zebrasporites fimbriatus* Bht-6 169.9 m. U. *Camarazonosporites rudis* V-1 276–278 m. V. *Camarazonosporites laevigatus* Bht-6 148.1 m. W. *Uvaesporites argentaeformis* V-1 326.0 m. X. *Triancoraesporites reticulatus* V-1 252.0 m. Y. *Baculatisporites comaumensis* Bht-6 148.1 m. Z. *Lycopodiacidites rugulatus* Bht-6 160.4 m. AA. *Cycadopites carpenteri* V-1 276–278 m. AB. *Micrhystridium breve* V-1 276–278 m. AC. *Cycadopites potonieii* V-1 252.0 m. AD–AE. *Aulisporites astigmosus* V-1 276–278 m. AF. *Lagenella martinii* V-1 276–278 m. AG. *Botryooccus braunii* V-1 276–278 m.

Lycopodiacidites kuepperi (Fig. 5H), *Lycopodiacidites rugulatus* (Fig. 5Z), *Uvaesporites gadensis* (Fig. 5D), *Kraeuselisporites cooksonae* (Fig. 5C), *Neoraistrickia taylorii* (Fig. 5J), *Verrucosisporites morulae* (Fig. 3M), *Trilites tuberculiformis* (Fig. 5M), *Conbaculatisporites mesozoicus* (Fig. 5O), *Baculatisporites comaumensis* (Fig. 5Y), *Rogalskaisporites cicatricosus* (Fig. 5E), *Anapiculatisporites telephorus* (Fig. 5G), *Porcellispora longdonensis* (Fig. 5K), *Zebrasporites kahleri* (Fig. 5L), *Z. fimbriatus* (Fig. 5T), *Striatella seebergensis* (Fig. 5N), *C. laevigatus* (Fig. 5V), and *Triancoraesporites reticulatus* (Fig. 5X). Monosaccate pollen (e.g., *Enzonalasporites vigens* Fig. 4M, P, *Patinasporites densus* Fig. 4O, *P. explanatus* Fig. 4N, *Vallasporites ignacii*) and Circumpolles (*Praecirculina granifer*) are still common constituents of the palynological assemblages forming about 10 % of the palynomorph sum respectively. Other pollen types e.g., *Lagenella martinii* (Fig. 5 AF), *Staurosaccites quadrifidus* (Fig. 4H, K), *Platysaccus queenslandi* (Fig. 4G), *Ovalipollis lunzensis* (Fig. 4I) or *Rimaesporites potoniei* (Fig. 4J) are constantly present, but in low numbers. Marine palynomorphs are very rare in this assemblage but the freshwater algae *Botryococcus braunii* (Fig. 5 AG) are commonly observed in the upper part of the Csicsó Marl albeit in low proportions. The same palynological assemblage is identified in the Balatonhenye Bht-6 core at 157.1–169.2 m and in the Barnag Bat-2 at 180–198 m (Fig. 8).

Palynological assemblages of the Sándorhegy Formation are best observed in the cores Balatonhenye Bht-6 and Barnag Bat-2 (Fig. 8). Three local assemblages are identified: the *densus-ignacii*-Circumpolles assemblage (Bht-6117–154.8 m and Bat-2 92–169.9 m), the *Aratrisporites-astigmosus-granifer* (Bht-6 39.5–51 m, Bat-2 from 57.3 to 89.1 m), and the uppermost *vigens-densus*-Circumpolles (Bht-6 28.6–34.8 m, Bat-2 20–53.5 m). The *Aratrisporites-astigmosus-granifer* assemblage is also identified in the Veszprém V-1 core at 159–164.5 m and the *vigens-densus*-Circumpolles assemblage is present at 141–154.5 m in the Veszprém V-1 borehole succession (Fig. 7).

The *densus-ignacii*-Circumpolles assemblage (Fig. 8, Bht-6 117–154.8 m, Bat-2 92–169.9 m) from the Pécsely Member of the Sándorhegy Formation is characterized by decreasing spore proportions (from 35 % down to <5 %) and increasing amount of alete bisaccate pollen, and monosaccate pollen with very high Circumpolles proportions that reach up to ~60 % in the Bat-2 core. The most frequent taxa are *Praecirculina granifer* (Fig. 6V), *Camerosporites secatus* (Fig. 6Y), *Duplicisporites continuus*, *D. scurrilis,* and *D. verrucosus* (Fig. 6W, Z). Marine palynomorphs reach higher relative proportions (~15 %) compared to the underlying assemblage of the Csicsó Marl. *Staurosaccites quadrifidus* (Figs. 4H and K) and *Ovalipollis* spp. (*O. minimus* Fig. 4L, *O. ovalis* Figs. 3J, 4C) form 5–10 % of the assemblages and some taxa, which were very rare in the Veszprém Formation e.g., *Ellipsovelatisporites plicatus* (Fig. 6J), becomes more common here.

Spores increase again in relative abundance (10–20 % in total) and diversity in the overlying *Aratrisporites-astigmosus-granifer* assemblage (Fig. 8, Bht-6 39.5–51 m, Bat-2 57.3–89.1 m) in the lower part of the Barnag Member with the most frequent taxa represented by *Aratrisporites* spp., *Deltoidospora,* and *Concavisporites*. Similar to the palynological assemblage of the Csicsó Marl Member, *Cycadopites* spp. co-occur with high relative abundances of *Aulisporites astigmosus* and very few *Riccisporites tuberculatus* specimens in this part of the Sándorhegy Formation. The abundance of marine palynomorphs particularly foraminifer tests, starts increasing in this interval reaching up to 40 % of the palynomorph sum.

The youngest palynological assemblage, the *vigens-densus*-Circumpolles (Figs. 7–8, Bht-6 28.6–34.8 m, Bat-2 20–53.5 m, and in the V-1 at 141–154.5 m) is characterized by the predominance of Circumpolles (*Camerosporites secatus, Praecirculina granifer*), and monosccate pollen (mainly *Patinasporites densus, Enzonalasporites vigens,* and *Vallasporites ignacii*) with increasing abundance of alete bisaccate pollen (e.g., *Hevizipollenites/Samaropollenites* indet. Figs. 6B–C, *Pityosporites devolvens* Fig. 6D, *Samaropollenites concinnus* Fig. 6E. Other taxa include *Podocarpidites keuperianus* (Fig. 6G), *Alisporites grauvogeli* (Fig. 6H), *Ellipsovelatisporites plicatus* (Fig. 6J), *Chordasporites singulichorda* (Fig. 6F). Furthermore, there is a declining trend of spore abundances (<5 %), accompanied by increases in the abundance of marine palynomorphs, particularly foraminiferal tests and the prasinophyte *Dictyotidium reticulatum* (Figs. 7–8).

4.2. Sporomorph ecogroups (SEGs), the hygrophyte/xerophyte (H/X), and intermediate/xerophyte ratios (I/X)

The SEG method reveals the overall dominance of the upland SEG, marine SEG, the dry lowland, and the *Alisporites* group (Table S5). In the lower part of Mencshely Marl (V-1 core) upland (average ~ 58 %, up to ~85 %) and marine SEG elements (average ~ 21 %, max. ~88 %) are predominant. Dry lowland, wet lowland, river and coastal SEG elements are very rare until 493 m (below 5 %) exhibiting a gradual increase in abundance between 493 and 485 m, but their ratios never exceed 10 % of the palynomorphs. Freshwater-brackish SEG elements are extremely scarce with only one horizon with increased relative abundances (2.4 %) at 485 m.

The Csicsó Marl Member (V-1 252–353 m, Bht-6 157.1–169.2 m, Bat-2 169.9–198 m) is characterized by a marked increase in the relative abundance of coastal (average ~ 10.4 %, max ~25 %), river (average ~ 7.6 %, max ~12.7 %), and dry lowland (average ~ 17.3 %, max ~33.2 %) SEG elements. The proportion of upland SEG elements is still high (above 50 %) in the lower part of the Csicsó Marl (V-1 338–353 m) but gradually decreases towards the upper part of the member. The relative abundance of the marine SEG component is markedly lower (max ~12.5 %) compared to the Mencshely Marl but starts increasing again in the uppermost part of the Csicsó Marl (Bat-2 169.9–180 m 8–10 %, Bht-6 157.1–169.2 m, 6–13 %). The freshwater-brackish component shows a slight increase in the Csicsó Marl up to ~3.2 % in V-1 and ~ 5 % in Bht-6.

In the lower part of the Sándorhegy Formation (Pécsely Member) in the *densus-ignacii*-Circumpolles assemblage (Bht-6117–154.8 m and Bat-2 92–169.9 m) upland SEG elements rise again from ~22 % to over 82 % of the palynological assemblage. Coastal, river and various lowland SEG elements are less common in this interval compared to the underlying Csicsó Marl usually below 10 % each. Marine SEG elements do not occur regularly, but they are increasing in abundance both in the Bat-2 (max 18 %) and Bht-6 cores (max ~66 %).

Lowland, river and coastal SEG elements attain again slightly higher relative abundances in the overlying *Aratrisporites-astigmosus-granifer* assemblage (Bht-6 39.5–51 m, Bat-2 57.3–89.1 m, V-1159–164.5 m), comprising up to 11 % in Bat-2, 29 % in Bht-6, and 81 % of the

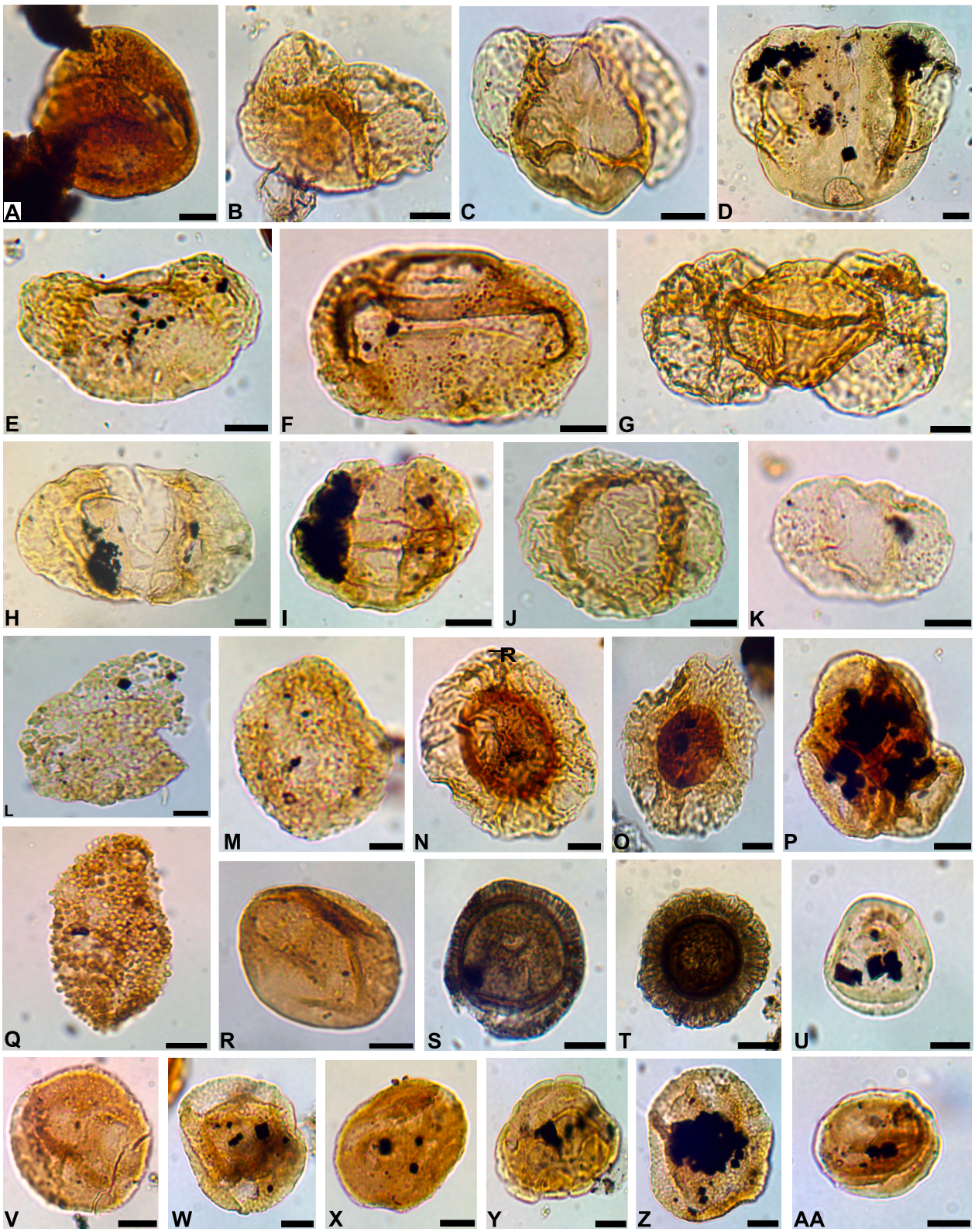

Fig. 6. Selected bisaccate, monosaccate, non-saccate, and Circumpolles pollen from the Sándorhegy Formation from boreholes Barnag Bat-2 and Balatonhenye Bht-6. The scale bar represents 10 μm for all figures. A. *Pityosporites devolvens* Bat-2 61–64 m. B. *Hevizipollenites/Samaropollenites* indet. Bat-2 83.6 m. C. *Hevizipollenites/Samaropollenites* indet. Bat-2 57.3 m. D. *Pityosporites devolvens* Bat-2 40.0 m. E. *Samaropollenites concinnus* Bat-2 40.0 m. F. *Chordasporites singulichorda* Bat-2 61–64 m. G. *Podocarpidites keuperianus* Bat-2 83.6 m. H. *Alisporites grauvogeli* Bat-2 53.5 m. I. *Lunatisporites acutus* Bat-2 94–102 m. J. *Ellipsovelatisporites plicatus* Bat-2 24.5 m. K. *Vitreisporites pallidus* Bat-2 61.0–64.0 m. L. cf. *Riccisporites tuberculatus* Bht-6 28.6 m. M. *Vallasporites ignacii* Bht-6 51.0 m. N. *Patinasporites densus* Bat-2 61.0–64.0 m. O *Patinasporites explanatus* Bht-6 51.0 m. P. *Partitisporites quadruplices* Bat-2 20.0 m. Q. cf. *Riccisporites tuberculatus* V-1 163.5 m. R. *Partitisporites tenebrosus* Bat-2 20.0 m. S. Reworked *Triadispora* sp. Bat-2 134.0 m. T. Reworked monosaccate pollen *Accintisporites* sp. sensu Roghi Bat-2 134.0 m. U. *Partitisporites maljawkinae* Bat-2 40.0 m. V. *Praecirculina granifer* Bat-2 57.3 m. W. *Duplicisporites verrucosus* Bat-2 20.0 m. X. *Partitisporites tenebrosus* Bht-6 24.8 m. Y. *Camerosporites secatus* Bat-2 94–102 m. Z. *Duplicisporites verrucosus* Bat-2 20.0 m. AA. *Partitisporites maljawkinae* Bht-6 51.0 m.

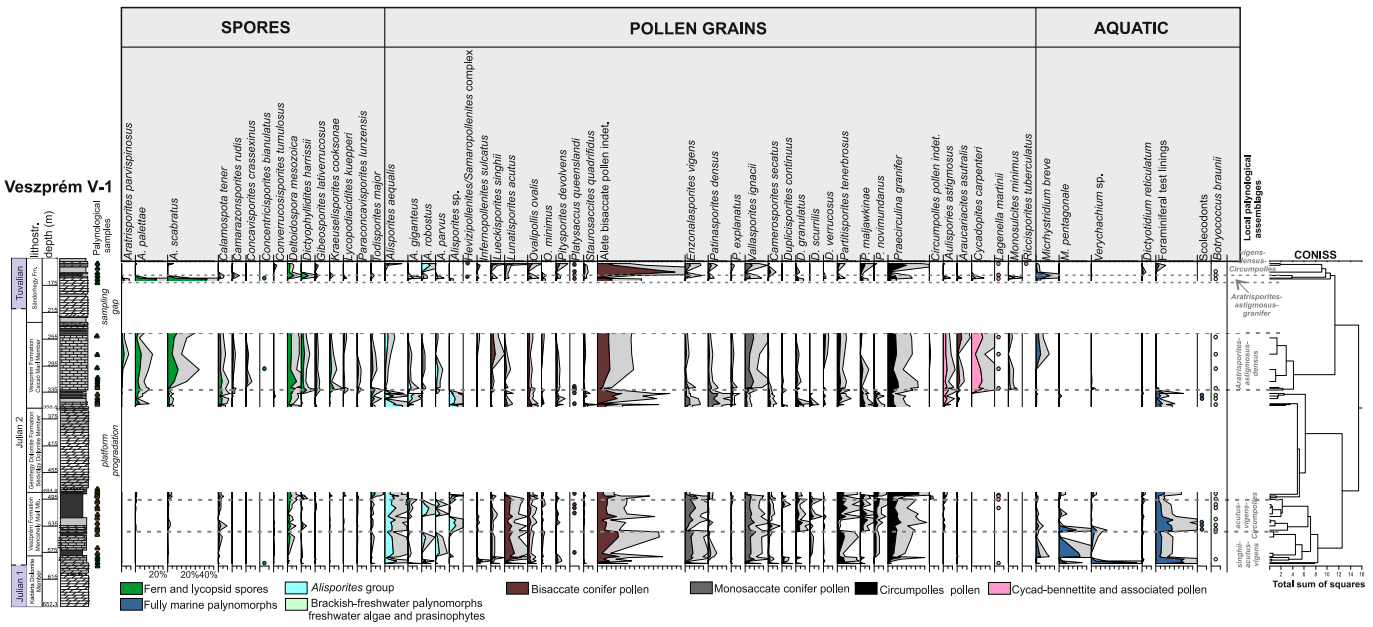

Fig. 7. Quantitative distribution of selected spore-pollen taxa and aquatic palynomorphs in the Veszprém V-1 borehole succession. Palynomorph abundance values are presented as percentage proportions (%) of the total spore-pollen sum. For rare taxa (abundance less <5 counts per sample) only presence-absence data are shown (circles). The grey field is the exaggeration (3×) of the relative abundances plotted in colour. To maintain clarity and readability of the diagram only selected taxa were plotted for this illustration. The complete diagram with all taxa can be found in the Supplementary material Fig. S1. For lithology see Fig. 2.

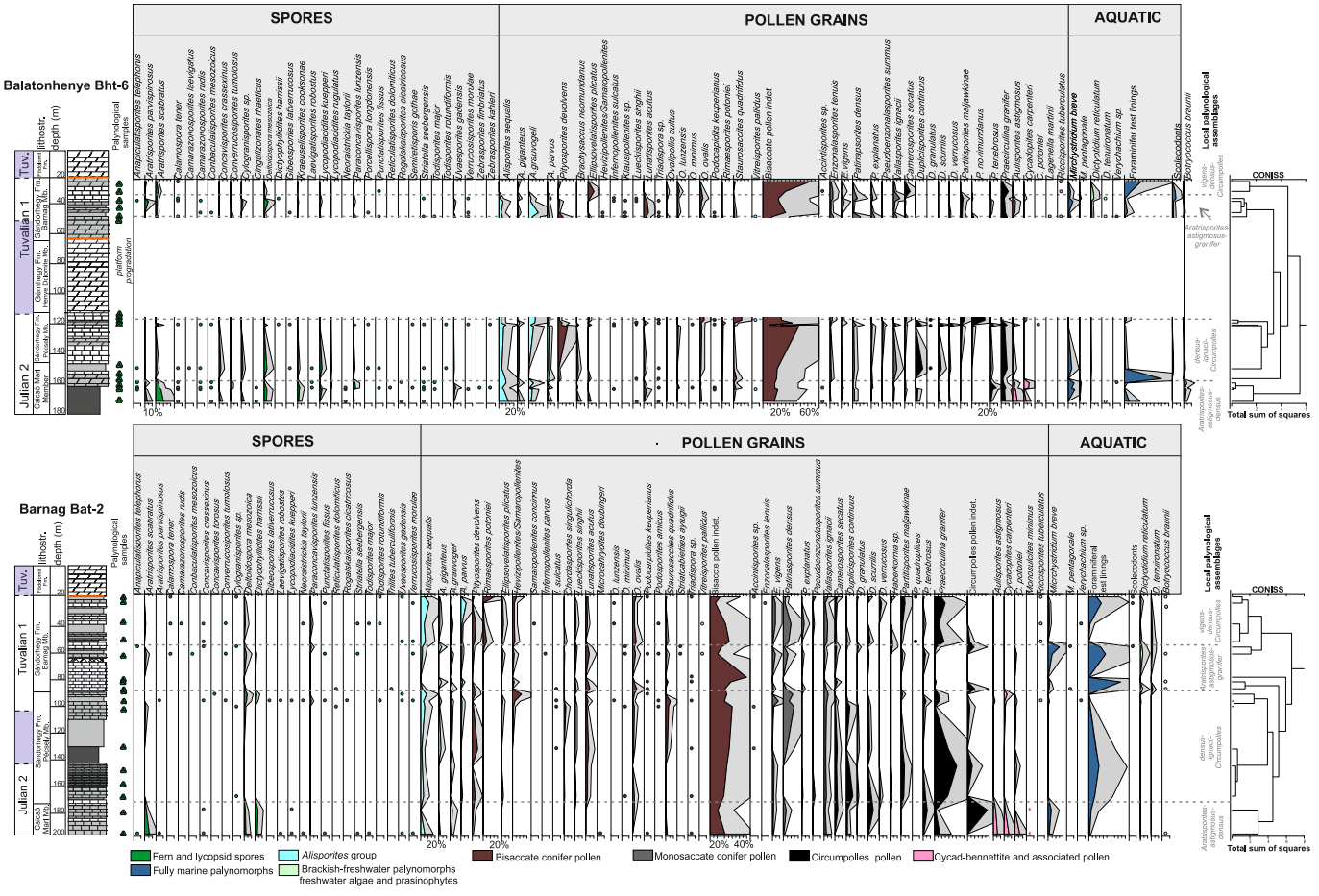

Fig. 8. Quantitative distribution of spore-pollen taxa and aquatic palynomorphs in the Balatonhenye Bht-6 and Barnag Bat-2 borehole successions. Palynomorph abundance values are presented as percentage proportions (%) of the total spore-pollen sum. For rare taxa (abundance less <5 counts per sample) only presence-absence data are shown (circles). The grey field is the exaggeration (3×) of the relative abundances plotted in colour. For lithology see Fig. 2.

palynological assemblage in V-1. As in the lower part of the Sándorhegy Formation, the topmost part of the borehole sequences represented by the local *densus-vigens*-Circumpolles assemblage (Bht-6 34.8–28.6 m, Bat-2 53.5–20 m, V-1154.5–141 m) is characterized again by the predominance of upland SEG elements (>50–80 %) and marine palynomorphs (up to 13–22 %).

The hygrophyte/xerophyte and intermediate/xerophyte ratio reflects the predominance of pollen taxa with xerophytic affinity in the entire succession with the exception of Csicsó Marl where moist loving and intermediate taxa increase in relative abundance evidenced by higher H/X and I/X values of ~1.1–1.5 and ~ 0.5–0.9 respectively (Supplementary Material Table S5, Figs. S2–S3). Additionally, several distinct hygrophyte and intermediate peaks are also recorded in the Mencshely Marl and Sándorhegy Formation (Supplementary Material Table S5, Figs. S2–S3).

5. Discussion

5.1. Palynostratigraphy

The lack of robust ammonoid or conodont-based age constraints required the integration of chemostratigraphy (Dal Corso et al., 2015, 2018) and selected palyno-events (Baranyi et al., 2019b) in order to correlate facies, climatic evolution, and biotic events in the Transdanubian Range with those across the Western Tethys. A broad negative carbon isotope excursion (NCIE) has been recorded in the uppermost part of the Füred Formation in the Balatonfüred Bfü-1 core that has been correlated to the onset of the globally synchronized CPE carbon cycle perturbation at the Julian 1–2 boundary (Dal Corso et al., 2015). However, in an adjacent borehole (Mencshely Met-1), the same NCIE was recorded in a bed that has already been assigned to the Veszprém Formation (Dal Corso et al., 2018) demonstrating a gradual transition from pelagic limestones to calcareous and clayey marls around the onset of the CPE (Fig. 2).

Concentricisporites bianulatus (Fig. 3F) was commonly found in the early Julian strata of the Predil and Rio del Lago formations extending into the Conzen Fromation in the Julian Alps and in the San Cassiano Formation of the Dolomites (Roghi, 2004; Dal Corso et al., 2018) with its latest occurrence usually confined to the *Trachyceras aonoides* subzone (Ulrichs, 1974; Van der Eem, 1983). This species is extremely rare in the investigated strata in the Transdanubian Range with a single occurrence in the deepest part of the Veszprém V-1 borehole succession at 588.35 m. The scarcity of this spore species may corroborate the chemostratigraphical correlation proposed by Dal Corso et al. (2015, 2018) suggesting that the age of the Veszprém Formation likely ranges from Julian 1 to Julian 2, and the boundary between Julian 1 and 2 is at the transition somewhere between the Füred and Veszprém formations or in the lower part of the Veszprém Formation. Based on the presence of *Duplicisporites continuus*, common occurrence of *Patinasporites densus, Partitisporites maljawkinae*, and *Camerosporites secatus* from the base of the studied succession, palynological assemblages of the Mencshely Marl can be correlated to the lower part of the *Duplicisporites continuus* assemblage (Roghi, 2004), the *densus-maljawkinae* phase by Van der Eem (1983) and the *Camerosporites secatus* phase from the Western

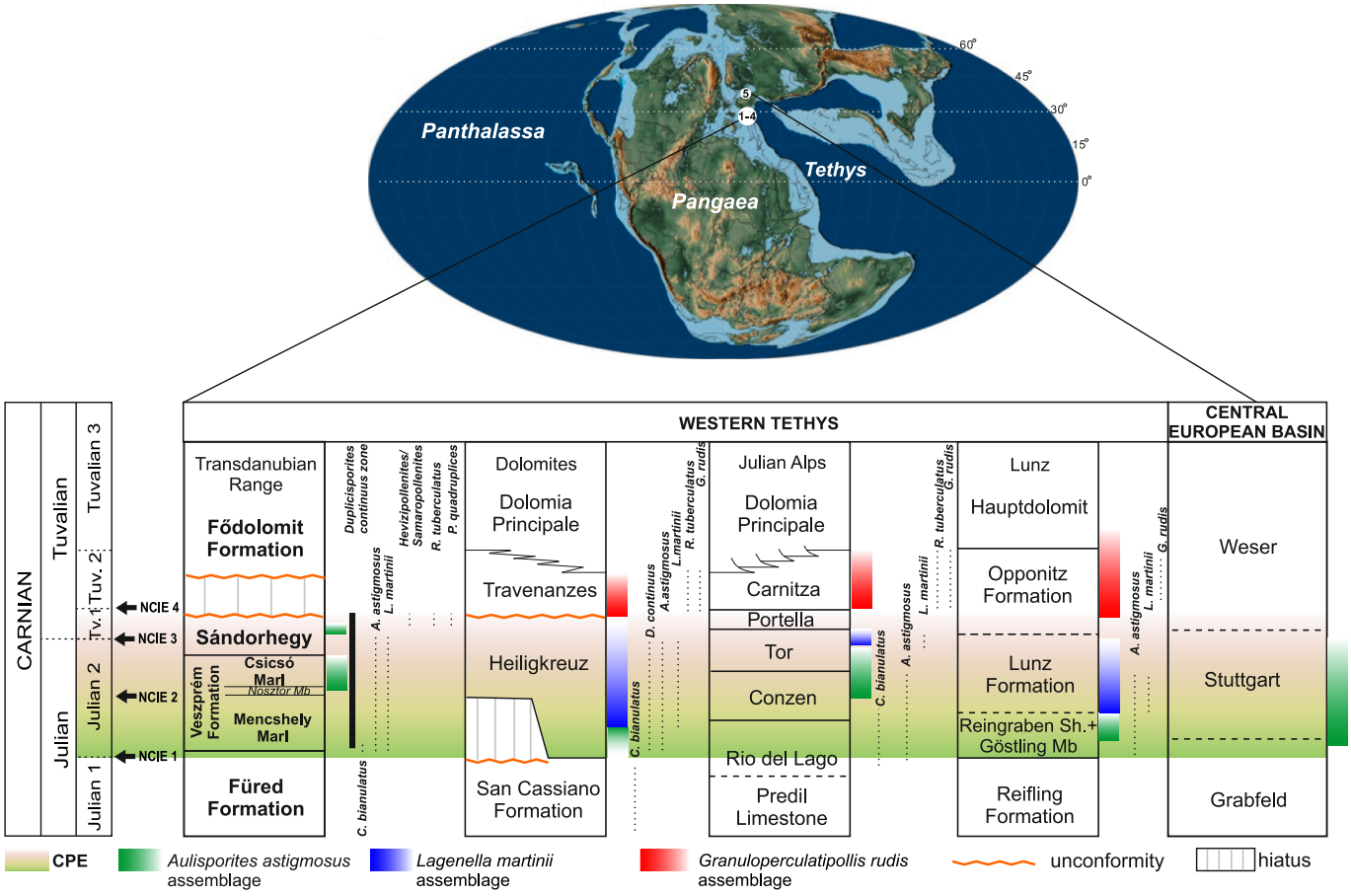

Fig. 9. Schematic lithostratigraphic chart of the Carnian formations in the studied areas in the Western Tethys realm and Central European Basin with the correlation of marker palynological assemblages and ranges of selected taxa. Modified after Dal Corso et al. (2018) and Jin et al. (2022). Map of the Carnian is from Scotese (2014), locations 1. Transdanubian Range, 2. Dolomites, 3. Julian Alps, 4. Lunz area, Northern Calcareous Alps, 5. Central European Basin. Palynological information is from Roghi (2004), Kürschner and Herngreen (2010), Roghi et al. (2010), Dal Corso et al. (2015, 2018), Mueller et al. (2016b), Baranyi et al. (2019b) and this study.

Tethys realm that corresponds to the entire Carnian (Visscher and Krystyn, 1978; Cirilli, 2010).

CPE deposits in the Western Tethys realm were characterized by three distinct palynological assemblages (Fig. 9) during the late Julian and early Tuvalian (*Aulisporites astigmosus, Lagenella martinii,* and the *Granuloperculatipollis rudis* assemblages) that have been used to correlate clastic pulses and climatic changes in this region and beyond (Roghi et al., 2010). The *Aulisporites astigmosus* assemblage corresponds to the lower part of the *Duplicisporites continnus* assemblage of Roghi (2004) which was distinguished as a miospore-acme zone (*Aulisporites-Aratrisporites* acme) with the predominance of the bennettite pollen *Aulisporites astigmosus* and lycopsid spores, particularly *Aratrisporites* spp., and the sphenophyte *Calamospora* (Fig. 9). This assemblage is markedly different from the early Julian (Cordevolian) palynofloras from the Alpine Tethys mainly with *C. secatus, D. granulatus, Enzonalasporites vigens, Patinasporites densus*, *Praecirculina granifer*, *Ovalipollis* spp. and *Triadispora* spp. (e.g., Van der Eem, 1983; Dunay and Fisher, 1978; Blendinger, 1988; Buratti and Carrillat, 2002). The assemblages with *Aulisporites* and many spore taxa were considered by Roghi (2004) and Roghi et al. (2010) as a good palynostratigraphical tool for correlating Carnian associations throughout Europe as it (or compositionally very similar assemblages) can be traced from the Alpine region e.g., Dolomites, Julian Alps, Karawanks, Lunz-area Austria, Eastern Alps, Lunzerschichten in the West Carpathians (e.g., Dunay and Fisher, 1978; Planderová, 1980; Hochuli and Frank, 2000; Roghi, 2004; Mueller et al., 2016b; Lukeneder et al., 2024), through the Central European Basin e.g., Schilfsandstein or Stuttgart Formation in Germany and Poland (Orłowska-Zwolińska, 1983, 1985; Fijałkowska-Mader et al., 2015; Visscher et al., 1994; Kürschner and Herngreen, 2010; Fijałkowska-Mader et al., 2015, 2021), and the Grès à Roseau in France (Adolff et al., 1984) to the Boreal Realm (e.g., Hochuli and Vigran, 2010; Paterson and Mangerud, 2015; Mueller et al., 2016a) correlated with the CPE interval. In the Cave del Predil area (Julian Alps), the acme of *Aulisporites* and various spore taxa (*Aratrisporites, Calamospora*) characterized a narrow interval from the upper Conzen Formation to the lower Tor Formation corresponding to the *Austrotrachyceras austriacum* and *Tropites dilleri* ammonoid zones (Broglio Loriga et al., 1999; Roghi, 2004) from the late Julian (or Julian 2) to early Tuvalian (Fig. 9). The same assemblage was also documented in the Reingraben Shales in the Lunz area (Northern Calcareous Alps, Mueller et al., 2016b) and in the lower part of the Heiligkreuz Formation in the Dolomites (Borca Member) where the presence of the ammonoids *Austrotrachyceras* sp. and *Sirenites senticosus* confirmed the Julian 2 age (Praehauser-Enzenberg, 1970; Roghi, 2004; Breda et al., 2009; Maron et al., 2017).

The *Lagenella martinii* assemblage (Fig. 9) with very high abundance of hygrophytic palynomorphs described from the first and second clastic units in the Raibl Beds and the middle-upper part of the Lunz Formation represents the second marker assemblage (Fig. 9) during the CPE subsequent to the acme of *A. astigmosus* and *Aratrisporites* (Jelen and Kušej, 1982; Roghi et al., 2010). The same assemblage was identified in the middle and upper part of the Tor Formation in the Cave del Predil area and in the Dibona Member of the Heiligkreuz Formation in the Dolomites with a Julian 2–Tuvalian 1 age range (Roghi et al., 2010; Maron et al., 2017).

Despite the fact that the first local occurrence of both *Aulisporites astigmosus* and *Lagenella martinii* were observed in the lower part of Mencshely Marl (Baranyi et al., 2019b, see also Fig. 2 of this study), sensu stricto neither the *Aulisporites astigmosus* nor the *Lagenella martinii* assemblage of Roghi et al. (2010) can be recognized in the CPE successions of the Transdanubian Range. Although present, both species are very rare in the studied samples at the onset of the CPE in the Mencshely Marl. However, characteristic elements of both the *Aulisporites astigmosus* and *Lagenella martinii* assemblages (e.g., *Aratrisporites, Concavisporites, Calamospora, Lycopodiacidites kuepperi, Patinasporites densus, Cycadopites* spp.) are very abundant in the overlying Csicsó Marl Member represented by the local *Aratrisporites-astigmosus-densus* assemblage in the late Julian 2 (Fig. 9).

The placement of the Julian–Tuvalian boundary is among the key questions in the biostratigraphical subdivision of the Carnian stage in the Transdanubian Range as this horizon is marked by the third distinct NCIE during the CPE (Dal Corso et al., 2018) and it is associated with the largest extinction rate across the event (Jenks et al., 2015; Dal Corso et al., 2020). It was previously placed in the lower part of the Sándorhegy Formation in the Balaton Highland by palynological constraints, foraminifer, and bivalve assemblages (Fig. 2, Góczán and Oravecz-Scheffer, 1996a, 1996b; Budai et al., 1999). The earlier palynological works of Góczán et al. (1983, 1991b) and Góczán and Oravecz-Scheffer (1996a, 1996b) did not record any marker taxa in the Sándorhegy Formation that are now considered to be indicative of the Tuvalian (see Cirilli, 2010; Kürschner and Herngreen, 2010 or Roghi, 2004; Roghi et al., 2010) such as *Ricciisporites tuberculatus, Granuloperculatipollis rudis* or *Classopollis meyerianus*. Góczán and Oravecz-Scheffer (1996a, 1996b) considered the first local occurrence of *Pseudoenzonalasporites summus* within the Sándorhegy Formation as the indicator of the Tuvalian substage. However, the species is present already from the early Carnian in the Northern Hemisphere (e.g., Cirilli, 2010). *Brodispora striata* was also listed as a characteristic Tuvalian element by Góczán and Oravecz-Scheffer (1996a, 1996b) due its occurrence in the Opponitz Formation (Dunay and Fisher, 1978) and Arden Sandstone in the UK (Clarke, 1965). However, this species is not restricted to the Tuvalian or even to the Carnian at all.

In the Julian Alps *Riccisporites tuberculatus* first appeared in the early Tuvalian (Roghi, 2004). This taxon was very rare in the Transdanubian Range, but sporadic occurrences were recorded in the upper part of Sándorhegy Formation (from 51 m in the Balatonhenye Bht-6, and from the sample 94–102 in Barnag Bat-2, and at 141–143 m in Veszprém V-1, see Fig. 2). *Samaropollenites specious* is also commonly recorded in late Carnian palynofloras in the Western Tethys realm (Visscher and Krystyn, 1978; Buratti and Carrillat, 2002; Roghi, 2004), Israel (Cirilli and Eshet, 1991) and Albania (Cirilli and Montanari, 1994), and assemblages with common *Camerosporites secatus, Vallasporites ignacii, Enzonalasporites vigens, Patinasporites densus, Partitisporites quadruplices,* and *Samaropollenites speciosus* were interpreted as Tuvalian in the Western Tethys (Visscher and Krystyn, 1978; Cirilli and Eshet, 1991; Cirilli and Montanari, 1994; Buratti and Carrillat, 2002). *Samaropollenites speciosus* was recorded first in the upper part of the Tor Formation in the Julian Alps (Roghi, 2004). Similar pollen types labelled as the *Hevizipollenites/Samaropollenites* complex were recorded in the upper part of the Sándorhegy Formation occurring from 159 to 160 m in Veszprém V-1, from 102.4 m in the Barnag Bat-2 boreholes, and from 51 m in Balatonhenye Bht-6 (Fig. 2). Its local first occurrence is recorded close to the first local occurrences of *R. tuberculatus* in all three boreholes pointing to a Tuvalian age for the Barnag Member above 102.4 m in Barnag Bat-2, above 51 m in the Balatonhenye Bht-6, and above 159–160 m in the Veszprém V-1 boreholes (Fig. 2).

The last occurrences of many key taxa e.g., *Lagenella martinii, Aulisporites astigmosus, Lunatisporites* spp., *Infernopollenites* spp., *Partitisporites maljawkinae, Vallasporites ignacii,* and *Duplicisporites continuus* are all recorded within the *Duplicisporites continuus* assemblage within the *Tropites dilleri* zone in the Julian Alps (Roghi, 2004). As the majority of these taxa are still present in the uppermost part of the Sándorhegy Formation (Figs. 7–8), the palynological assemblages from both the Veszprém and Sándorhegy formations in the Transdanubian Range are correlated to the *Duplicisporites continuus* assemblage zone. Although facies correlation is not a guarantee for the same age, but the upper part of the Barnag Member is very similar in facies variation to the uppermost part of the Heiligkreuz Formation, the Lagazuoi Member (Budai et al., 1999), in addition to that both formations are capped by an emersion surface and hiatus (Breda et al., 2009; Breda and Preto, 2011; Pecorari et al., 2023). In the upper part of the Heiligkreuz Formation, the ammonoids *Shastites* cf. *pilari* and cf. *Jovites* sp. and conodonts *Paragondolella noah,* and *Metapolygnathus praecommunisti* indicated an early

Tuvalian age correlated to the *Tropites dilleri* zone (Breda et al., 2009; Maron et al., 2017). Thus, based on analogies from the Dolomites, the upper part of the Sándorhegy Formation is likely still early Tuvalian.

In the third clastic unit of the Raibl Beds as well as in the lower part of the Opponitz Formation, monosaccate pollen (*Enzonalasporites* group) and Circumpolles became prevalent assigned to the *Granuloperculatipollis rudis* assemblage calibrated in the Julian Alps to the Tuvalian 2–3 (Roghi, 2004; Roghi et al., 2010). *Granuloperculatipollis rudis* appears first in the *Tropites subbulatus* zone (Roghi, 2004) and the assemblage with its predominance has been recorded from both the Carnitza (Julian Alps) and Travenanzes formations in the Dolomites (Roghi, 2004; Roghi et al., 2010) yet this species was not observed in the Transdanubian Range. The lack of this marker species, together with the presence of *Duplicisporites continuus, Partitisporites maljawkinae, Aulisporites astigmosus,* and *Lagenella martinii*, in the upper part of the Barnag Member indicates still an early Tuvalian age. The absence of the *Granuloperculatipollis rudis* assemblage also confirms the well-known hiatus between the Sándorhegy and Fődolomit Formation (Dolomia Principale equivalent in the Transdanubian Range), that likely includes the time interval of the *G. rudis* assemblage. Unfortunately, there are no biostratigraphically significant marker taxa observed in the basal layers of the Fődolomit Formation in the Balaton Highland to constrain the extent of the stratigraphical gap, but the megalodontid fauna with *Neomegalodon triqueter pannonicus, N. carinthiacus,* and *N. guembeli*, from the Aranyos Valley outcrop of the Fődolomit Formation near Veszprém (Végh-Neubrandt, 1982), points to a Tuvalian onset of its deposition. Depositional units, which are age and facies-equivalent with the Carnitza, Travenanzes and parts of the Opponitz Formation, separating the CPE deposits and the Dolomia Principale equivalent deposits, are missing in the Transdanubian Range due to this hiatus (Budai et al., 1999). Notably, there are indications of unconformity at the base of both the Travenanzes and Carnitza formations as well (Breda et al., 2009; Breda and Preto, 2011; Gale et al., 2015) that corresponds to a regional sequence boundary of a third order eustatic cycle in the Western Tethys (Gianolla et al., 1998a, 2021). Specifically, in the Balaton Highland, dolomite breccias, reddish-brown sediments at the connection of the Sándorhegy and Fődolomit Formation are indicative of a longer phase of subaerial exposure with uplift and erosion before the deposition of the Fődolomit commenced (Budai et al., 1999; Budai and Haas, 1997; Budai et al., 1999).

5.2. Vegetation change during the Carnian Pluvial Episode (CPE) based on the palynological assemblages

As a consequence of the assumed humid climate shift at the onset of the CPE, wet habitats and hygrophytic plant associations and riparian-deltaic habitats expanded in the Western Tethys realm (e.g., Roghi, 2004; Pott et al., 2008; Roghi et al., 2010, 2022; Mueller et al., 2016b), yet both the macro- and micro plant remains hosted still many conifers generally attributed with xerophytic affinity. Palynomorphs in marginal marine sediments of Western Tethys originated from an extensive catchment area including plants of moist lowland and riparian habitats together with pollen of hinterland/upland vegetation from well drained areas further from watercourses (Kustatscher et al., 2018; Roghi et al., 2022). This mixing is also evident in the palynological records with diverse conifer pollen assemblages usually associated with hinterland and more arid conditions and rich spore associations indicative of lush lowland environments (e.g., Roghi et al., 2022).

The negative carbon isotope excursion at the Julian 1 and Julian 2 marks the beginning of the C-cycle perturbation associated with the CPE and a notable increase in hygrophytic vegetation elements as well as the expansion of riparian and lacustrine deltaic floras in the Western Tethyan realm (e.g., Roghi, 2004; Roghi et al., 2010, 2022; Mueller et al., 2016b; Lukeneder et al., 2024). A strong increase in the abundance of hygrophytic palynomorphs was observed between the upper part of the Conzen Formation to the top of the Tor Formation in the Julian Alps, in the Heiligkreuz Formation in the Dolomites, and in the Reingraben Formation in the Lunz area of the Northern Calcareous Alps (see *A. astigmosus* and L. *martinii* assemblages in Fig. 9, Roghi, 2004; Roghi et al., 2010, 2022; Mueller et al., 2016b).

Considering the currently available biostratigraphical and chemostratigraphical data from the Transdanubian Range (Dal Corso et al., 2015, 2018), the onset of the CPE coincides with the increase in clastic influx and the transition from a carbonate (Füred Formation) to a mixed clastic-carbonate depositional style represented by the Veszprém Formation (Rostási et al., 2011; Haas et al., 2012). Yet in the Transdanubian Range, in the lower part of the Veszprém Formation (Mencshely Marl) the palynological assemblages are still dominated by upland SEG elements including Majonicaceae, Voltziaceae, and possibly Cheirolepidiaceae with minor contribution from lowland to coastal vegetation element like lycopsids, ferns, and possibly seed ferns (Fig. 10). The producers of the *Alisporites* group, conifers and/or seed ferns, could have populated upland as well as lowland, riverine, swamp and even mangrove-like habitats (e.g., Popa and Van Konijnenburg-van Cittert, 2006; Barbacka, 2011; Gee et al., 2020).

The Voltziaceae and Majonicacae conifers in the Late Triassic were generally thought to have xerophytic affinity and they grew on drier ground, well-drained soils further from the watercourses (Roghi et al., 2022), with pollen transported mainly by wind to the hemipelagic basins of the Transdanubian Range. The *Enzonalasporites* group (including *Vallasporites* and *Patinasporites*) were likely produced by voltzialean, Majonicaceae or other early conifers, and interestingly, these taxa peaked in global abundance during the CPE period (Sciborski et al., 2022). This observation seemingly contrasts with the general ecological interpretation of a xerophytic affinity for these conifer pollen (Visscher and Van der Zwan, 1981). Roghi et al. (2022) reconciled the conflict between the sedimentological (i.e. elevated terrestrial influx) and palynological climate proxies by interpreting the high abundance of Cheirolepidiaceae and Majonicaceae as an indication of halophytic plant assemblages that colonized coastal areas with constant physiological drought due to excessive salt in the water, soils, and air but which were not necessarily arid. On the other hand, Sciborski et al. (2022) suggested that the parent plants of *Enzonalasporites* group were probably voltzialean conifers that used a pollination drop for their germination that represents an adaptation to arid climate (Runions and Owens, 1996; Nepi et al., 2012). Yet they argued that the development of the drop required at least temporally (seasonally) humid conditions. Consequently, the parent plants of these pollen preferred not arid but strongly seasonal climate under the influence of a monsoonal climatic regime with episodic or periodic high levels of moisture (Sciborski et al., 2022).

This palynological observation also emphasizes the climatic interpretation of the CPE by Kozur and Bachmann (2010), Stefani et al. (2010), and Mueller et al. (2016b) suggesting that the climate history during the CPE was a phase with several humid pulses such as episodic/periodic intense monsoon periods, rather than just a shift to uniformly humid conditions. The C-cycle perturbation associated with the CPE likely intensified the Pangean megamonsoon circulation (Kutzbach and Gallimore, 1989; Parrish, 1993). A similar trend of increased monsoon intensity with higher interannual variability in precipitation and increased frequency of extremely wet monsoon seasons with very intense rainfall, has recently been observed in East Asia as a modern response to the ongoing climate change and global warming (e.g., Katzenberger et al., 2021, 2022; Moon et al., 2023). A similar scenario can be easily envisaged for the CPE that could lead to strongly seasonal and seasonally wet climate particularly at the beginning of the CPE in the Western Tethys that secured the proper conditions for the proliferation of the *Enzonalasporites* (*Vallasporites,* and *Patinasporites* included) producers. Also, the seasonally heavy rainfall could have washed in a large amount of upland/hinterland SEG pollen types into the various depositional basins such as lakes and/or marine basins, providing an explanation for the high relative abundance of upland pollen in the early CPE deposits (e.g., Bonis et al., 2010; Baranyi et al., 2019a, 2024).

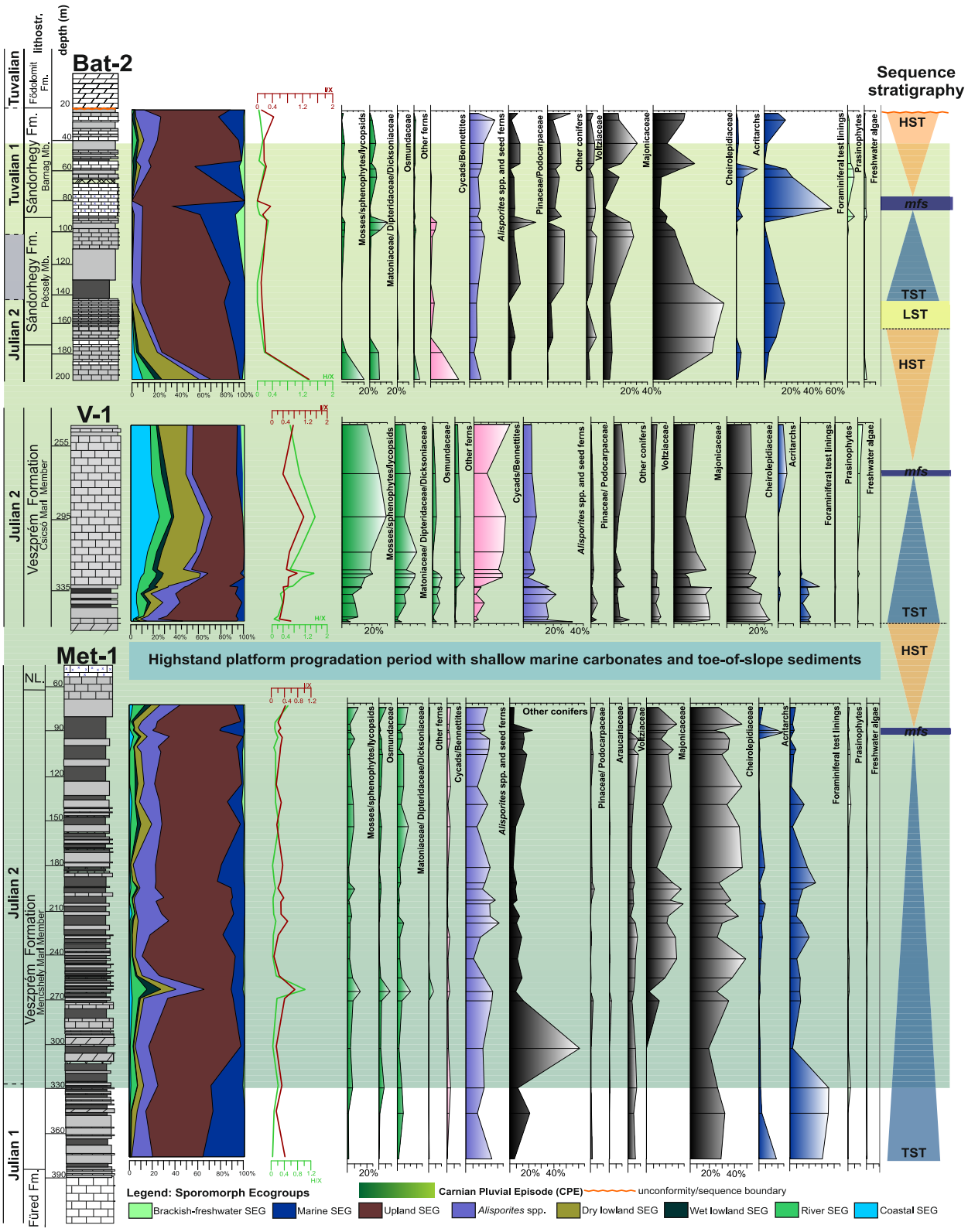

Fig. 10. Vegetation history and changes in the environmental (SEG groups) and climatic proxies in the Transdanubian Range during the Carnian Pluvial Episode. Palynofloral trends reflect the variation between major botanical groups. Note that the charts are compiled from the composite dataset of the Mencshely Met-1 (Baranyi et al., 2019b), Veszprém V-1 and Barnag Bat-2 borehole data. For a more comprehensive view on the early Julian 2 vegetation patterns the SEG data of the Mencshely Met-1 borehole was also provided from Baranyi et al. (2019b) that gives a more detailed insight into the onset of the CPE. The complete SEG and climate proxy data for boreholes Veszprém V-1 and Balatonhenye Bht-6 are given in the Supplementary Material figs. S2–S3. Sequence stratigraphy interpretation is after Budai and Haas (1997) and Haas and Budai (1999). Abbreviations: HST = highstand system tract, TST = transgressive system tract, LST = lowstand system tract, mfs = maximum flooding surface. For lithology see Fig. 2.

The lack of clear humid signal simultanosuly with the NCIE and C-cycle perturbation also emphasizes that the climate change might not have been synchronous or everywhere evenly developed as there are still many locations in Western Europe where a clear shift to more humid climate is absent or ambiguous in the palynological data (e.g., Franz et al., 2019; Lindström et al., 2017; Baranyi et al., 2019a). However, the similarities between Carnian palynofloras in the Alpine Realm (Dolomites, Northern Calcareous Alps, Transdanubian Range) indicates that the continental source area for the dispersed palynomorphs is closely related implying that the climate change at least within that region should be comparable. The siliciclastic material of the Veszprém Formation was likely derived from the Val Sabbia Sandstone or similar lithostratigraphic units in the Lombardian continental area (Budai et al., 1999), but the source of the spore and pollen was likely more complex during the CPE, including areas of the European and Gondwana shelves (Góczán and Oravecz-Scheffer, 1996a, 1996b) with increasing catchment size during the CPE (e.g., Pecorari et al., 2023). There are several well-known Carnian macorfloras in the Alpine Realm e.g., the Lunz, Monte Pora and Raibl plant assemblages (e.g., Kustatscher et al., 2018), which were likely a key source for the palynological assemblages in the Transdanubian Range. The Lunz Formation in particular preserved a diverse swamp habitat e.g., with many ferns, cycads/bennettitales with less common occurence of sphenophytes, conifers and putative ginkgophytes while the Italian and Slovenian floral assemblages were dominated by conifers belonging to the allochtonous floral elements that lived further away from the watercourses (Dobruskina, 1998, 2001; Pott et al., 2008; Pott and Krings, 2010; Kustatscher et al., 2018).

In the Transdanubian Range only the palynological assemblage of the Csicsó Marl indicate the clear presence of wet lowland mire forest vegetation and deltaic riparian habitats similar to the Lunz flora (Fig. 10). Hygrophytic spores together with cycad (*Cycadopites* spp.) and bennettite-related (*Aulisporites astigmosus*) pollen also reached an acme during the deposition of this lithostratigraphic unit within the CPE interval (Fig. 10). Dipteridaceae, Matoniaceae, Dicksoniaceae, and to a lesser extent Osmundaceae ferns, lycopsids together with sphenophytes (horsetails) were forming the ground cover of the vegetation, while the mid-canopy was inhabited by cycads, bennettites, and possibly seed ferns (Li et al., 2020, 2022). The acme of *Aratrisporites* was interpreted as the establishment of a mangrove-like ecosystem (Roghi et al., 2010) in the coastal areas (Fig. 10). Large lacustrine systems could have developed globally due to the substantial rise in precipitation during the CPE (e.g., McKie, 2014; Mancuso et al., 2020; Lu et al., 2021; Pecorari et al., 2023), that led probably to changes in coastal landscape as well with the formation of extensive wetland habitats. Yet the development of the new vegetation types that produced lycopsid and fern spores, and hosted cycads, and bennettites likely required some time after the onset of the CPE explaining the delay in the expression of the humid climate and why only the Csicsó Marl reflects the colonisation of riparian forests and lowland marshes. This scenario can also incorporate the presence of halophytic plant assemblages with cheirolepids and other conifers as suggested by Roghi et al. (2022) before and in the early stages of the CPE, that was later transformed into wetlands as the climate change progressed.

Alpine palynofloras recorded a second compositional shift in the middle to late Tuvalian in the late phase and the aftermath of the CPE with a trend of increasing Circumpolles abundances and diversity, and increases in the relative abundance of Pinaceae and Podocarpaceae conifers (e.g., Roghi et al., 2010; Kustatscher et al., 2018; Dal Corso et al., 2020). In the Transdanubian Range, the stratigraphical gap on top of the Sándorhegy Formation likely encompassed the time interval of the middle to late Tuvalian (*Granuloperculatipollis rudis* assemblage), thus the immediate recovery of the CPE cannot be detected here. Yet, there were increases in the relative abundance of Pinaceae and Podocarpaceae conifers (*Pityosporites, Hevizipollenites/Samaropollenites,* and *Podocarpidites*) in the Sándorhegy Formation compared to the underlying Veszprém Formation together with a significant drop in taeniate bissacates (*Lunatisporites*, *Lueckisporites*, and *Infernopollenites*) in the early Tuvalian. This compositional shift in conifer proportions already foreshadowed a major floristic change occurring in late Carnian and Norian, particularly the proliferation and diversification of Circumpolles pollen (Kürschner and Herngreen, 2010; Kustatscher et al., 2018; Dal Corso et al., 2020; Roghi et al., 2022).

5.3. Simultanous effects of climate change and sea-level variations

Certain features of the palynological assemblages e.g., the over-representation of upland SEG pollen and oscillation in the relative proportion of marine palynomorphs in the lower Mencshely Marl as well as in the Sándorhegy Formation (Fig. 10), might imply that other environmental parameters exerted a control on the composition of palynofloras besides climate change. Sea-level rise could lead to the over-representation of upland SEG pollen in distal marine or transgressive beds due to the selective transportation of saccate pollen grains into an offshore depositional setting and drowning of coastal lowlands, where spores and cycad/bennettite pollen would have originated ("Neves Effect", Chaloner, 1958; Chaloner and Muir, 1968; Tyson, 1995; Abbink et al., 2004; Kustatscher et al., 2010). The Carnian is marked by several transgressive-regressive cycles in the Western Tethys (Gianolla et al., 1998a, 2021; Stefani et al., 2010; Gattolin et al., 2015; Tekin et al., 2024). Similarly, the deposition of the Mencshely Marl in the early Julian 2 was also associated with a transgressive cycle (Sequence C1, Budai and Haas, 1997; Haas and Budai, 1999) that could explain the high abundance of monosaccate, taeniate, and alete bisaccate pollen in the palynological assemblages (Fig. 10). The first increase in the hygrophyte/xerophyte ratio coincided with the first negative isotope excursion around 325.9 m in the Met-1 core (Dal Corso et al., 2018), hinting a link between climate, vegetation, and carbon cycle but the proportion of hygrophytic palynomorphs remained small in the lower part of the Mencshely Marl (Fig. 10). The oscillations in the relative abundance of marine palynomorphs and spores, belonging to the lowland, riverine, and coastal ecogroups both in the V-1 and Met-1 cores (Figs. 10 and S2), indicate that the terrestrial supply was not constant and that local sea level rise exerted an equally significant control on the composition of palynological assemblages. The maximum flooding surface of the Sequence C1 transgression is placed below the platform carbonates (Sédvölgy Member) or deeper water limestones, represented by the Nosztor Limestone Member in the uppermost part of the Mencsehely Marl (Budai and Haas, 1997; Haas and Budai, 1999) which was also indicated by a sudden peak in acritarchs and foraminiferal test lining abundances in both boreholes (Figs. 10, S2, see also Baranyi et al., 2019b).

Interestingly, the deposition of the Csicsó Marl was again simultaneous with the onset of a new transgressive cycle (Sequence C2, Budai and Haas, 1997; Haas and Budai, 1999). However, during the deposition of this unit the climatic changes led to the establishment of the source areas for hygrophytic plants and lowland (wetland, riparian, deltaic) habitats. Consequently, their palynomorph assemblages were transported to the marine sites in the Transdanubian Range due to the enhanced hydrological cycling and terrestrial influx leading to the upfilling of the hemipelagic basins (Rostási et al., 2011; Haas et al., 2012; Baranyi et al., 2019b; Pecorari et al., 2023).

Although, the assemblages in the Sándorhegy Formation are still correlated to the CPE interval (late Julian 2–early Tuvalian, Figs. 2 and 9), the quantitative composition of the palynomorph assemblages does not unequivocally show humid climatic conditions in the Transdanubian Range (Fig. 10). The relative abundance of monosaccate, taeniate bisaccate, and Circumpolles pollen, forming the upland SEG with xerophytic affinity, started rising in the Pécsely Member represented by the local *densus-ignacii*-Circumpolles assemblage (Figs. 8 and 10). In other parts of the Western Tethys, in the lowermost Opponitz Formation *Aratrisporites* spp. and *Aulisporites astigmosus* started decreasing, but a dramatical drop in the hygrophytic groups and increase of monosaccate

(*Enzonalasporites* spp., *Patinasporites* spp., *Vallasporites ignacii*), taeniate bisaccate (*Lunatisporites acutus* Fig. 4F), and Circumpolles pollen was observed only later from the lower-middle part of the Opponitz Formation parallel with a rise in marine palynomorphs (Roghi et al., 2010; Mueller et al., 2016b). In the Julian Alps and in the Dolomites, a clear increase in xerophytic pollen (mainly Circumpolles) and a drop in spore and cycad/bennettite abundances was only observed in the younger Tuvalian Carnitza and Travenanzes formations, suggesting aridification at the end of the CPE (Breda and Preto, 2011). Following this analogy, the observed palynological trend with the decrease of hygrophytic flora could be interpreted as a return to overall drier climatic conditions in the Transdanubian Range as early as the latest Julian 2, accompanied by the return of carbonate-dominated deposition in the lower Sándorhegy Formation (Nagy, 1999; Nagy and Csillag, 2002; Haas et al., 2012). However, considering the available age constraint and the correlation of the Sándorhegy to the Heiligkreuz and Tor formations (e.g., Budai et al., 1999), caution has to be taken when interpreting the Hungarian palynological data as an earlier, late Julian 2 return of drier climate. Notwithstanding, the presence and presumed episodic expansions of wet habitats characterizing the CPE interval, were still recorded in the Transdanubian Range but only by isolated peaks of cycad, bennettite pollen (<5 % of the spore-pollen sum) and hygrophytic spore peaks (up to 20 %) in the Barnag Member (upper Sándorhegy Formation, local *Aratrisporites-astigmosus-granifer* assemblage, Figs. 7–8 and 10). There were also a lot more variations detected in the relative abundance of marine palynomorphs in the entire Sándorhegy Formation (Figs. 10 and S3) warranting that besides climate a secondary environmental parameter such as sea-level variations also influenced the composition of palynofloras during the late Julian and earliest Tuvalian.

According to the sequence stratigraphical interpretation of the Sándorhegy Formation, a large part of the formation represents an individual transgressive-regressive cycle (Budai and Haas, 1997; Haas and Budai, 1999). The lower part of the Pécsely Member above the bituminous limestones records the onset of a new transgression (Sequence C3) indicated by the deposition of bioclastic carbonates (Budai and Haas, 1997; Haas and Budai, 1999) that coincided with a rise in conifer pollen and marine taxa in the palynological assemblages (local *densus-ignacii*-Circumpolles assemblage, Figs. 8, 10 and S3). This new transgressive cycle likely caused the drowning of coastal marshes, leading to the overrepresentation of xerophytic upland SEG pollen (i.e., conifers) again leading to a bias towards wind-transported palynomorphs. The maximum flooding surface of this cycle was placed at the cherty limestone horizon at the base of the Barnag Member (Budai and Haas, 1997; Nagy and Csillag, 2002, see Fig. 2) coincident with a sudden increase in the abundance of the foraminiferal tests in Bat-2 at 83.6–89.1 m. Subsequently, the successions of both the Barnag Bat-2 and Balatonhenye Bht-6 cores showed an upward shallowing trend in the Barnag Member consistent with a highstand system tract deposition (HST, Budai and Haas, 1997; Nagy, 1999; Nagy and Csillag, 2002). The marly intercalations with higher relative abundance of hygrophytic palynomorphs (spores) and cycad-bennettite pollen within the Barnag Member (at 61.3–64.3 m, 57.3 m, and 40 m, Figs. 10 and S3) evidenced the continued presence of wet habitats on land and the considerable transport of lowland sporomorphs due to relative proximity of the shoreline during the highstand period.

A more convincing evidence for aridification with the decrease of hygrophytic palynomorphs and the decrease of terrestrial input, is only found in the uppermost part of the Barnag Member represented by the *vigens-densus*-Circumpolles assemblage (Figs. 10 and S3, Bht-6 28.6–34.8 m, Bat-2 20–24.5 m, and V-1141–154.5 m). Since it was deposited during the same highstand period, similar to the underlying *Aratrisporites-astigmosus-granifer* local assemblage, a climatic change is required as for the cause of the observed changes in the palynofloras. Similarly, the ostracod assemblages in this part of the Barnag Member below the unconformity horizon (Tóth et al., 2024), are also enriched in thick-walled ornamented shallow water taxa that delivers additional evidence for the recovery or carbonate factories and decrease of clastic influx.

In summary, our new data confirm that sea-level changes and the variations in terrestrial influx were superimposed on global climatic trends. The palynological data shed light on a complex interplay between regional and global processes. Humid pulses and transgressions acted in tandem and both of them markedly influenced the quantitative composition of the palynofloras in the Transdanubian Range during the Carnian Pluvial Episode.

6. Conclusions

Palynological data from three Carnian borehole successions in the Transdanubian Range (Western Hungary) revealed the vegetation patterns and climate history during the Carnian Pluvial Episode.

- The Veszprém and Sándorhegy Formation span the late Julian (Julian 2) to early Tuvalian and their palynological assemblages correspond to the *Duplicisporites continuus* zone from the Julian Alps and Dolomites representing the Julian 2 and early Tuvalian interval. Equivalent assemblages to the *Auliporites astigmosus* and *Lagenella martinii* assemblages from the Alpine Realm are restricted to the Csicsó Marl in the late Julian 2 even though the marker species are present in low numbers from the base of the Veszprém Formation. The absence of the marker species *Granuloperculatipollis rudis, Classopollis meyerianus,* and the low abundance of *Riccisporites tuberculatus* in the Barnag Member indicates that the topmost part of the Sándorhegy Formation is still early Tuvalian. The time interval represented by the *Granuloperculatipollis rudis* assemblage from the Julian Alp and Lunz area is missing in the Transdanubian Range due to a pronounced hiatus between the Sándorhegy and Fődolomit Formation.
- Local eustatic sea level variation and the effect of the more distal depositional setting of the Transdanubian Range were superimposed on the global climate trends that influenced the distribution and relative abundance of various palynomorph groups. Transgressive episodes at the onset of the CPE and close to the Julian–Tuvalian boundary promoted the transport of the wind-blown monosaccate, bisaccate, and Circumpolles pollen with xerophytic affinity by contrast to the fluvially transported spores and cycad/bennettite pollen.
- Pronounced increases in hygrophyte plants, together with peaks of the river and lowland SEG taxa, are confined to the Csicsó Marl Member and isolated occurrences in the upper part of the overlying Sándorhegy Formation suggesting that the climate change is not uniform or everywhere evenly developed. The proliferation of the *Enzonalasporites* group (*Vallasporites*, and *Patinasporites* included) might point to strongly seasonal and seasonally wet climate at the beginning of the CPE in the Western Tethys.
- The increase in xerophyte pollen indicates aridification, decrease of clastic influx, and the waning of the pluvial phase in the uppermost part of the Sándorhegy Formation in the early Tuvalian. The complete return of arid conditions and recovery in the aftermath of CPE is not detected due to a hiatus.

Declaration of generative AI in scientific writing

During the preparation of this work the author(s) used DeepL Write in order to improve the style and language of the manuscript. After using this tool/service, the author(s) reviewed and edited the content as needed and take(s) full responsibility for the content of the published article.

CRediT authorship contribution statement

Viktória Baranyi: Writing – original draft, Methodology,

Investigation, Formal analysis, Data curation, Conceptualization. **Tamás Budai:** Writing – review & editing. **Viktor Karádi:** Writing – review & editing. **Xin Jin:** Writing – review & editing. **Wolfram M. Kürschner:** Writing – review & editing. **Emőke Tóth:** Writing – review & editing, Funding acquisition.

Funding

This work was supported by the internal research project „WEGETA" at the Croatian Geological Survey, funded by the National Recovery and Resilience Plan 2021–2026 of the European Union – NextGenerationEU; and the National Research, Development and Innovation Office of Hungary (NKFIH FK 134229).

Declaration of competing interest

The authors declare that they have no known competing financial interests or personal relationships that could have appeared to influence the work reported in this paper.

Acknowledgements

We thank our Editor Howard Falcon-Lang for the handling of our manuscript, as well as we express our gratitude to Mihai Emilian Popa, Evelyn Kustatscher, Anna Mader, Elke Schneebeli, and one anonymous reviewer for their thorough and constructive criticism that helped improve this study. The research was conducted within the scope of the internal research project „WEGETA" at the Croatian Geological Survey, funded by the National Recovery and Resilience Plan 2021–2026 of the European Union – NextGenerationEU, monitored by the Ministry of Science, Education and Youth of the Republic of Croatia. The research received financial support from the National Research, Development and Innovation Office of Hungary (NKFIH FK 134229 grant). Emőke Tóth was supported by the János Bolyai Research Scholarship of the Hungarian Academy of Sciences and the ÚNKP-23-5 new national excellence program of the Ministry for Culture and Innovation from the source of the National Research, Development and Innovation Fund. We are grateful for Dragica Kovačić (Croatian Geological Survey) for performing the palynological processing. This work is a contribution to IGCP 739.

Appendix A. Supplementary data

Supplementary data to this article can be found online at https://doi.org/10.1016/j.palaeo.2025.112989.

Data availability

Data will be made available on request.

References

Abbink, O.A., Van Konijnenburg-van Cittert, J.H.A., Visscher, H., 2004. A sporomorph ecogroup model for the Northwest European Jurassic - lower cretaceous: concepts and framework. Netherlands J. Geosc. 83, 17–38.
Adolff, M.C., Appia, C., Doubinger, J., Lienhardt, M.J., 1984. Zonations palynostratigraphiques dans les séries triasiques traversées par des sondages dans le Jura et le Bas-Dauphiné. Géol. Fr. 1-2, 3–21.
Baranyi, V., Miller, C.S., Ruffell, A., Hounslow, M.W., Kürschner, W.M., 2019a. A continental record of the Carnian Pluvial Episode (CPE) from the Mercia Mudstone Group (UK): palynology and climatic implications. J. Geol. Soc. Lond. 176, 149–166.
Baranyi, V., Rostási, Á., Raucsik, B., Kürschner, W.M., 2019b. Palynology and weathering proxies reveal climatic fluctuations during the Carnian Pluvial Episode (CPE) (Late Triassic) from marine successions in the Transdanubian Range (western Hungary). Glob. Planet. Chang. 177, 157–172.
Baranyi, V., Jin, X., Dal Corso, J., Li, B.B., Kemp, D.B., 2024. Vegetation response to climate change during an early Jurassic hyperthermal event (Jenkyns Event) from Northern China (Ordos Basin). Palaeogeogr. Palaeoclimatol. Palaeoecol. 643, 112180.
Barbacka, M., 2011. Biodiversity and the reconstruction of early Jurassic Flora from the Mecsek Mountains (southern Hungary). Acta Palaeobotan. 51 (2), 127–179.
Barrenechea, J.F., López-Gómez, J., De La Horra, R., 2018. Sedimentology, clay mineralogy and palaeosols of the Mid-Carnian Pluvial Episode in eastern Spain: insights into humidity and sea-level variations. J. Geol. Soc. Lond. 175, 993–1003.
Batten, D.J., 2002. Chapter 26A Palynofacies and petroleum potential. In: Jansonius, J., McGregor, D.C. (Eds.), Palynology: Principles and Applications, Vol. 3. American Association of Stratigraphic Palynologists Foundation, Dallas, Texas, pp. 1065–1084.
Bernardi, M., Gianolla, P., Petti, F.M., Mietto, P., Benton, M.J., 2018. Dinosaur diversification linked with the Carnian Pluvial Episode. Nat. Commun. 9, 1499.
Birks, H.J.B., Birks, H.H., Ammann, B., 2016. The fourth dimension of vegetation. Science 354, 412–413.
Blendinger, E., 1988. Palynostratigraphy of the late Ladinian and Carnian in the Southeastern Dolomites. Rev. Palaeobot. Palynol. 53, 329–348.
Bonis, N.R., Ruhl, M., Kürschner, W.M., 2010. Milankovitch-scale palynological turnover across the Triassic–Jurassic transition at St. Audrie's Bay, SW UK. J. Geol. Soc. Lond. 167, 877–888.
Breda, A., Preto, N., 2011. Anatomy of an Upper Triassic Continental to Marginal-Marine System: the mixed Siliciclastic-Carbonate Travenanzes Formation (Dolomites, Northern Italy). Sedimentology 58, 1613–1647.
Breda, A., Preto, N., Roghi, G., Furin, S., Meneguolo, R., Ragazzi, E., Fedele, P., Gianolla, P., 2009. The Carnian Pluvial Event in the Tofane Area (Cortina d'Ampezzo, Dolomites, Italy). Geo.Alp. 6, 80–115.
Broglio Loriga, C., Cirilli, S., De Zanche, V., di Bari, D., Gianolla, P., Laghi, G.F., Lowrie, W., Manfrin, S., Mastandrea, A., Mietto, P., Muttoni, G., Neri, C., Posenato, R., Rechichi, M.C., Rettori, R., Roghi, G., 1999. The Prati di Stuores/Stuores Wiesen Section (Dolomites, Italy): a candidate Global Stratotype Section and Point for the base of the Carnian stage. Riv. Ital. Paleontol. Stratigr. 105, 37–78.
Budai, T., Haas, J., 1997. Triassic sequence stratigraphy of the Balaton Highland, Hungary. Acta Geol. Hung. 40 (3), 307–335.
Budai, T., Vörös, A., 1993. The Middle Triassic events of the Transdanubian Central Range in the frame of the Alpine evolution. Acta Geol. Hung. 36 (1), 3–13.
Budai, T., Vörös, A., 2006. Middle Triassic platform and basin evolution of the Southern Bakony Mountains (Transdanubian Range, Hungary). Riv. Ital. Paleontol. Stratigr. 112 (3), 359–371.
Budai, T., Császár, G., Csillag, G., Dudko, A., Koloszár, L., Majoros, Gy, 1999. Geology of the Balaton Highland. Explanation to the Geological Map of the Balaton Highland, 1: 50000. Occ. Papers Geol. Inst. Hung. 197, 169–257.
Buratti, N., Carrillat, A., 2002. Palynostratigraphy of the Mufara Formation (Middle–Upper Triassic, Sicily). Riv. Ital. Paleontol. Stratigr. 108, 101–117.
Chaloner, W.G., 1958. The Carboniferous upland flora. Geol. Mag. 95, 261–262.
Chaloner, W.G., Muir, M., 1968. Spores and floras. In: Murchison, D., Westoll, T.S. (Eds.), Coal and Coal-Bearing Strata. Oliver & Boyd, Edinburgh, pp. 127–146.
Cirilli, S., 2010. Upper Triassic-lowermost Jurassic palynology and palynostratigraphy: A review. In: Lucas, S.G. (Ed.), The Triassic Timescale, vol. 334. Geological Society of London Special Publication, pp. 221–262.
Cirilli, S., Eshet, Y., 1991. First discovery of *Samaropollenites* and the Onslow Microflora in the Upper Triassic of Israel, and its phytogeographic implications. Palaeogeogr. Palaeoclimatol. Palaeoecol. 85, 207–212.
Cirilli, S., Montanari, L., 1994. The evaporitic Carnian succession from Bistrica river (southern Albany). Paleopelagos 4, 107–118.
Clarke, R.F.A., 1965. Keuper miospore from Worcestershire, England. Palaeontology 8 (2), 294–321.
Csillag, G., Földvári, M., 2005. Upper Triassic amber fragments from the Balaton Highland, Hungary. Magyar Állami Földtani Inézet Évi Jelentése 2005-ről, pp. 37–46 (in Hungarian, with English Abstract).
Csontos, L., Vörös, A., 2004. Mesozoic plate tectonic reconstruction of the Carpathian region. Palaeogeogr. Palaeoclimatol. Palaeoecol. 210, 1–56.
Dal Corso, J., Mietto, P., Newton, R.J., Pancost, R.D., Preto, N., Roghi, G., Wignall, P.B., 2012. Discovery of a major negative $\delta^{13}C$ spike in the Carnian (late Triassic) linked to the eruption of Wrangellia flood basalts. Geology 40, 79–82.
Dal Corso, J., Gianolla, P., Newton, R.J., Franceschi, M., Roghi, G., Caggiati, M., Raucsik, B., Budai, T., Haas, J., Preto, N., 2015. Carbon isotope records reveal synchronicity between carbon cycle perturbation and the "Carnian Pluvial Event" in the Tethys realm (Late Triassic). Glob. Planet. Chang. 127, 79–90.
Dal Corso, J., Gianolla, P., Rigo, M., Franceschi, M., Roghi, G., Mietto, P., Manfrin, S., Raucsik, B., Budai, T., Jenkyns, H.C., Reymond, C.E., Caggiati, M., Gattolin, G., Breda, A., Merico, A., Preto, N., 2018. Multiple negative carbon-isotope excursions during the Carnian Pluvial Episode (Late Triassic). Earth-Sci. Rev. 185, 732–750.
Dal Corso, J., Bernardi, M., Sun, Y., Song, H., Seyfullah, L.J., Preto, N., Gianolla, P., Ruffell, A., Kustatscher, E., Rhogi, G., Merico, A., Hohn, S., Schmidt, A.R., Marzoli, A., Newton, R.J., Wignall, P.B., Benton, M.J., 2020. Extinction and dawn of the modern world in the Carnian (late Triassic). Sci. Adv. 6, eaba0099.
Dobruskina, I.A., 1998. Lunz flora in the Austrian Alps: a standard for Carnian floras. Palaeogeogr. Palaeoclimatol. Palaeoecol. 143, 307–345.
Dobruskina, I.A., 2001. Upper Triassic Flora from "Raibl beds" of Julian Alps (Italy) in Karavanke Mts. (Slovenia). Geologija 44, 263–290.
Dosztály, L., Kovács, S., Budai, T., 1989. Pécsely, Meggy hegy quarry. In: XXI European Micropalaeontological Colloquium, Guidebook.
Dunay, R.E., Fisher, M.J., 1978. The Karnian palynoflora succession in the Northern Calcareous Alps, Lunz am See, Austria. Pollen Spores 20 (1), 177–187.
Fijałkowska-Mader, A., Heunischn, C., Szulc, J., 2015. Palynostratigrpahy and palynofacies of the Upper Silesian Keuper (Southern Poland). Ann. Soc. Geol. Pol. 85, 637–661.
Fijałkowska-Mader, A., Jewuła, K., Bodor, E., 2021. Record of the Carnian Pluvial Episode in the polish microflora. Palaeoworld 30, 106–125.

Forte, G., Kustatscher, E., Ragazzi, E., Roghi, G., 2022. Amber droplets in the Southern Alps (NE Italy): a link between their occurrences and main humid episodes in the Triassic. Riv. Ital. Paleontol. Stratigr. 128, 105–127.
Franz, M., Kustatscher, E., Heunisch, C., Niegel, S., Röhling, H.-G., 2019. The Schilfsandstein and its flora; arguments for a humid mid-Carnian episode? J. Geol. Soc. Lond. 176, 133–148.
Furin, S., Preto, N., Rigo, M., Roghi, G., Gianolla, P., Crowley, J.L., Bowring, S.A., 2006. High-precision U-Pb zircon age from the Triassic of Italy: implications for the Triassic time scale and the Carnian origin of calcareous nannoplankton and dinosaurs. Geology 34, 1009–1012.
Gale, L., 2012. Rhaetian foraminiferal assemblage from the Dachstein Limestone of Mt. Begunjščica (Košuta Unit, eastern Southern Alps). Geologija 55, 17–44.
Gale, L., Celarc, B., Caggiati, M., Kolar-Jurkovšek, T., Jurkovšek, B., Gianolla, P., 2015. Paleogeographic significance of Upper Triassic basinal succession of the Tamar Valley, northern Julian Alps (Slovenia). Geol. Carpath. 66, 269–283.
Gattolin, G., Preto, N., Breda, A., Franceschi, M., Isotton, M., Gianolla, P., 2015. Sequence Stratigraphy after the Demise of a High-Relief Carbonate Platform (Carnian of the Dolomites): Sea-Level and climate Disentangled. Palaeogeogr. Palaeoclimatol. Palaeoecol. 423, 1–17.
Gee, C.T., Anderson, H.M., Anderson, J.M., Ash, S.R., Cantrill, D.J., Van Konijnenburg-van Cittert, J.H.A., Vajda, V., 2020. Postcards from the Mesozoic: Forest landscapes with giant flowering trees, enigmatic seed ferns, and other naked-seed plants. In: Martinetto, E., Tschopp, E., Gastaldo, R.A. (Eds.), Nature through Time. Springer Textbooks in Earth Sciences, Geography and Environment. Springer, Cham, pp. 159–185.
Gianolla, P., De Zanche, V., Mietto, P., 1998a. Triassic sequence stratigraphy in the Southern Alps (Northern Italy): definition of sequences and basin evolution. SEPM Spec. Publ. 60, 719–747.
Gianolla, P., Roghi, G., Ragazzi, E., 1998b. Upper Triassic amber in the Dolomites (Northern Italy). A paleoclimatic indicator? Riv. Ital. Paleontol. Stratigr. 104, 381–390.
Gianolla, P., Caggiati, M., Riva, A., 2021. The interplay of carbonate systems and volcanics: Cues from the 3D model of the Middle Triassic Sciliar/Schlern platform (Dolomites, Southern Alps). Mar. Pet. Geol. 124, 104794.
Góczán, F., Oravecz-Scheffer, A., 1996a. Tuvalian sequences of the Balaton Highland and the Zsámbék Basin, part I: Litho-, bio- and chronostratigraphic subdivision. Acta Geol. Hung. 39 (1), 1–31.
Góczán, F., Oravecz-Scheffer, A., 1996b. Tuvalian sequences of the Balaton Highland and the Zsámbék Basin, Part II: Characterization of sporomorph and foraminifer assemblages, biostratigraphic, palaeogeographic and geohistoric conclusions. Acta Geol. Hung. 39 (1), 33–101.
Góczán, F., Haas, J., Lőrincz, H., Oravecz-Scheffer, A., 1983. Faciological and stratigraphic evaluation of a Carnian key section (borehole Hévíz 6, Keszthely Mts, Hungary). In: Magyar Állami Földtani Inézet Évi Jelentése 1981-ről, pp. 263–293 (in Hungarian with English Abstract.).
Góczán, F., Oravecz-Scheffer, A., Csillag, G., 1991a. The stratigraphic characterization of the Cordevolian and Julian Formations of Csukréti Ravine, Balatoncsicsó. Magyar Állami Földtani Inézet Évi Jelentése 1989-ról, pp. 241–323.
Góczán, F., Oravecz-Scheffer, A., Csillag, G., 1991b. The stratigraphic characterization of the Cordevolian and Julian Formations of Csukréti Ravine, Balatoncsicsó. Földt. Int. Évi Jel. 1989-ról, pp. 241–323.
Grimm, E.C., 1987. CONISS: a FORTRAN 77 program for stratigraphically constrained cluster analysis by the method of incremental sum of squares. Comput. Geosci. 13, 13–35.
Haas, J., Budai, T., 1995. Upper Permian-Triassic facies zones in the Transdanubian Range. Riv. Ital. Paleontol. Stratigr. 101, 249–266.
Haas, J., Budai, T., 1999. Triassic sequence stratigraphy of the Transdanubian Range (Hungary). Geol. Carpath. 50 (6), 459–475.
Haas, J., Budai, T., 2014. Stratigraphic and facies problems of the Upper Triassic in the Transdanubian Range reconsideration of old problems on the basis of new results. Földtani Közlöny 144, 125–142 (in Hungarian, with English Abstract).
Haas, J., Kovács, S., Krystyn, L., Lein, R., 1995. Significance of late Permian–Triassic facies zones in terrane reconstructions in the Alpine–North Pannonian domain. Tectonophysics 242, 19–40.
Haas, J., Budai, T., Piros, O., Szeitz, P., Görög, Á., 2010. Late Triassic platform, slope and basin deposits in the Pilis Hills, Transdanubian Range, Hungary. Centr. Europ. Geol. 53 (2–3), 233–260.
Haas, J., Budai, T., Raucsik, B., 2012. Climatic controls on sedimentary environments in the Triassic of the Transdanubian Range (Western Hungary). Palaeogeogr. Palaeoclimatol. Palaeoecol. 353, 31–44.
Hochuli, P.A., Frank, S.M., 2000. Palynology (dinoflagellate cysts, spore-pollen) and stratigraphy of the lower Carnian Raibl Group in the Eastern Swiss Alps. Eclogae Geol. Helv. 93, 429–443.
Hochuli, P.A., Vigran, J.O., 2010. Climate variations in the Boreal Triassic—Inferred from palynological records from Barents Sea. Palaeogeogr. Palaeoclimatol. Palaeoecol. 290, 20–42.
Hornung, T., Brandner, R., Krystyn, L., Joachimski, M.M., Keim, L., 2007. Multistratigraphic constraints on the NW Tethyan "Carnian crisis". In: Lucas, S.G., Spielmann, J.A. (Eds.), The Global Triassic, 41, pp. 59–67.
Hu, Y., Li, X., Boos, W.R., Guo, J., Lan, J., Lin, Q., Han, J., Zhang, J., Bao, X., Yuan, S., Wei, Q., Liu, Y., Yang, J., Nie, J., Guo, Z., 2023. Emergence of the modern global monsoon from the Pangaea megamonsoon set by palaeogeography. Nat. Geosci. 16, 1041–1046.
Jelen, B., Kušej, J., 1982. Quantitative palynological analysis of Julian clastic rocks from the lead –zinc deposit of Mežica. Geologija 25, 213–227.
Jenks, J.F., Monnet, C., Balini, M., Brayard, A., Meier, M., 2015. Biostratigraphy of Triassic Ammonoids. In: Klug, C., Korn, D., De Baets, K., Kruta, I., Mapes, R.H. (Eds.), Ammonoid Paleobiology: From Macroevolution to Paleogeography. Springer, Netherlands, Dordrecht, pp. 329–388.
Jin, X., Gianolla, P., Shi, Z., Franceschi, M., Caggiati, M., Du, Y., Preto, N., 2020. Synchronized changes in shallow water carbonate production during the Carnian Pluvial Episode (late Triassic) throughout Tethys. Glob. Planet. Chang. 184, 103035.
Jin, X., Franceschi, M., Martini, R., Shi, Z., Gianolla, P., Rigo, M., Wall, C.J., Schmitz, M. D., Lu, G., Du, Y., Huang, X., Preto, N., 2022. Eustatic sea-level fall and global fluctuations in carbonate production during the Carnian Pluvial Episode. Earth Planet. Sci. Lett. 594, 117698.
Jin, X., Tomimatsu, Y., Yin, R., Onoue, T., Franceschi, M., Grasby, S.E., Du, Y., Rigo, M., 2023. Climax in Wrangellia LIP activity coincident with major Middle Carnian (late Triassic) climate and biotic changes: Mercury isotope evidence from the Panthalassa pelagic domain. Earth Planet. Sci. Lett. 607, 118075.
Katzenberger, A., Schewe, J., Pongratz, J., Levermann, A., 2021. Robust increase of Indian monsoon rainfall and its variability under future warming in CMIP6 models. Earth Syst. Dynam. 12, 367–386.
Katzenberger, A., Levermann, A., Schewe, J., Pongratz, J., 2022. Intensification of very wet monsoon seasons in India under global warming. Geophys. Res. Lett. 49, e2022GL098856.
Klaus, W., 1960. Sporen der karnischen Stufe der ostalpinen Trias. In: Jahrbuch der Geologischen Bundesanstalt Sonderband, 5, pp. 107–184.
Kozur, H.W., Bachmann, G.H., 2010. The Middle Carnian Wet Intermezzo of the Stuttgart Formation (Schilfsandstein), Germanic Basin. Palaeogeogr. Palaeoclimatol. Palaeoecol. 290, 107–119.
Kürschner, W.M., Herngreen, G.F.W., 2010. Triassic palynology of central and northwestern Europe: A review of palynological diversity patterns and biostratigraphic subdivisions. In: Lucas, S.G. (Ed.), The Triassic Timescale, vol. 334. Geological Society of London Special Publication, pp. 263–283.
Kustatscher, E., Van Konijnenburg-van Cittert, J.H.A., Roghi, G., 2010. Macrofloras and palynomorphs as possible proxies for palaeoclimatic and palaeoecological studies: a case study from the Pelsonian (Middle Triassic) of Kühwiesenkopf/Monte Prà della Vacca (Olang Dolomites, N-Italy). Palaeogeogr. Palaeoclimatol. Palaeoecol. 290, 71–80.
Kustatscher, E., Heunisch, C., Van Konijnenburg-van Cittert, J.H.A., 2012. Taphonomical implications of the Ladinian megaflora and palynoflora from Thale (Germany). Palaios 27, 753–764.
Kustatscher, E., Ash, S.R., Karasev, E., Pott, C., Vajda, V., Yu, J., McLoughlin, S., 2018. Flora of the Late Triassic. In: Tanner, L.H. (Ed.), The Late Triassic World, Topics in Geobiology, 46. Springer, Cham, pp. 545–622.
Kutzbach, J.E., Gallimore, R.G., 1989. Pangaean climates: Megamonsoons of the megacontinent. J. Geophys. Res. 94, 3341–3357.
Li, L., Wang, Y.D., Kürschner, W.M., Ruhl, M., Vajda, V., 2020. Palaeovegetation and palaeoclimate changes across the Triassic–Jurassic transition in the Sichuan Basin, China. Palaeogeogr. Palaeocl. 556, 109891.
Li, L., Kürschner, W.M., Lu, N., Chen, H., An, P., Wang, Y., 2022. Palynological record of the Carnian Pluvial Episode from the northwestern Sichuan Basin, SW China. Rev. Palaeobot. Palynol. 304, 104704.
Lindström, S., Erlström, M., Piasecki, S., Nielsen, L.H., Mathiesen, A., 2017. Palynology and terrestrial ecosystem change of the Middle Triassic to lowermost Jurassic succession of the eastern Danish Basin. Rev. Palaeobot. Palynol. 244, 65–95.
Lu, J., Zhang, P.X., Dal Corso, J., Yang, M.F., Wignall, P.B., Greene, S.E., Shao, L.Y., Lyu, D., Hilton, J., 2021. Volcanically driven lacustrine ecosystem changes during the Carnian Pluvial Episode (late Triassic). Proc. Natl. Acad. Sci. USA 118, e2109895118.
Lukeneder, A., Lukeneder, P., Sachsenhofer, R.F., Roghi, G., Rigo, M., 2024. Multi-proxy record of the Austrian Upper Triassic Polzberg Konservat-Lagerstätte in light of the Carnian Pluvial Episode. Sci. Rep. 14, 11194.
Mancuso, A.C., Benavente, C.A., Irmis, R.B., Mundil, R., 2020. Evidence for the Carnian Pluvial Episode in Gondwana: new multiproxy climate records and their bearing on early dinosaur diversification. Gondwana Res. 86, 104–125.
Maron, M., Muttoni, G., Dekkers, M.J., Mazza, M., Roghi, G., Breda, A., et al., 2017. Contribution to the Magnetostratigraphy of the Carnian: New Magneto-Biostratigraphic Constraints from Pignola-2 and Dibona Marine Sections, Italy, 50, pp. 187–203.
Mazaheri-Johari, M., Gianolla, P., Mather, T.A., Frieling, J., Chu, D., Dal Corso, J., 2021. Mercury deposition in Western Tethys during the Carnian Pluvial Episode (Late Triassic). Sci. Rep. 11, 17339.
McKie, T., 2014. Climatic and tectonic controls on Triassic dryland terminal fluvial system architecture, Central North Sea. In: Martinius, A.W., Ravnås, R., Howell, J.A., Steel, R.J., Wonham, J.P. (Eds.), Depositional Systems to Sedimentary Successions on the Norwegian Continental Margin, International Association of Sedimentologists. John Wiley & Sons, Chichester, West Sussex, pp. 19–58.
Miller, C.S., Peterse, F., da Silva, A.-C., Baranyi, V., Reichart, G.J., Kürschner, W.M., 2017. Astronomical age constraints and extinction mechanisms of the late Triassic Carnian crisis. Sci. Rep. 7, 2557.
Moon, S., Utsumi, N., Jeong, J-H., Yoon, J-H., Simon Wang, S.-Y., Shiogama, H., Kim, H., 2023. Anthropogenic warming induced intensification of summer monsoon frontal precipitation over East Asia Sci. Adv. 9, eadh4195.
Moore, P.D., Webb, J.A., Collinson, M.E., 1991. Pollen Analysis. Blackwell Scientific Publications, Oxford, p. 216.
Mueller, S., Hounslow, M.W., Kürschner, W.M., 2016a. Integrated stratigraphy and palaeoclimate history of the Carnian Pluvial Event in the Boreal realm; new data from the Upper Triassic Kapp Toscana Group in Central Spitsbergen (Norway). J. Geol. Soc. Lond. 173, 186–202.

Mueller, S., Krystyn, L., Kürschner, W.M., 2016b. Climate variability during the Carnian Pluvial phase — a quantitative palynological study of the Carnian sedimentary succession at Lunz am See, Northern Calcareous Alps, Austria. Palaeogeogr. Palaeoclimatol. Palaeoecol. 441, 198–211.
Nagy, Z.S.R., 1999. Platform-basin transition and depositional models for the Upper Triassic (Carnian) Sándorhegy Limestone, Balaton Highland. Acta Geol. Hung. 42, 267–299.
Nagy, Z.S.R., Csillag, G., 2002. Correlation of Upper Julian to Lower Tuvalian (Carnian) depositional cycles from the Balatonhenye–Barnag area, Balaton Highland, Hungary. Acta Geol. Hung. 45 (1), 45–62.
Nepi, M., von Aderkas, P., Pacini, E., 2012. Sugary exudates in plant pollination. In: Vivanco, J., Baluška, F. (Eds.), Secretions and Exudates in Biological Systems. Signaling and Communication in Plants, vol. 12. Springer, Berlin, Heidelberg, pp. 155–185.
Ogg, J.G., 2015. The mysterious Mid-Carnian "Wet Intermezzo" global event. J. Earth Sci. 26, 181–191.
Orłowska-Zwolińska, T., 1983. Palynostratigraphy of the Upper part of Triassic epicontinental sediments in Poland. Pr. Inst. Geol. 104, 1–89 (In Polish, with English summary).
Orłowska-Zwolińska, T., 1985. Palynological zones of the polish epicontinental Triassic. Bull. Polish Acad. Sci. Earth Sci. 33, 107–119.
Parrish, J.T., 1993. Climate of the supercontinent Pangea. J. Geol. 101, 215–233.
Paterson, N.W., Mangerud, G., 2015. Late Triassic (Carnian-Rhaetian) palynology of Hopen, Svalbard. Rev. Palaeobot. Palynol. 220, 98–119.
Paterson, N.W., Mangerud, G., Mørk, A., 2016. Late Triassic (early Carnian) palynology of shallow stratigraphical core 7830/5-U-1, offshore Kong Karls Land, Norwegian Arctic. Palynology 41 (2), 230–254.
Pecorari, M., Caggiati, M., Dal Corso, J., Cruciani, G., Tateo, F., Chu, D., Gianolla, P., 2023. Weathering and sea level control on siliciclastic deposition during the Carnian Pluvial Episode (Southern Alps, Italy). Palaeogeogr. Palaeoclimatol. Palaeoecol. 617, 111495.
Peng, J., Slater, S.M., Vajda, V., 2022. A Late Triassic vegetation record from the Huangshanjie Formation, Junggar Basin, China: possible evidence for the Carnian Pluvial Episode. Geol. Soc. Lond. Spec. Publ. 521, 95–108.
Planderová, E., 1980. Palynomorphs from Lunz Beds and from black clayey shales in basement of Vienna Basin (borehole LNV-7). Geol. Carpath. 31, 267–294.
Popa, M.E., Van Konijnenburg-van Cittert, J.H.A., 2006. Aspects of Romanian Early-Middle Jurassic palaeobotany and palynology. Part VII. Successions and floras. Prog. Nat. Sci. 16, 203–212.
Pott, C., Krings, M., 2010. Gymnosperm foliage from the Upper Triassic of Lunz, Lower Austria: an annotated checklist and identification key. Geol. Alps 7, 19–38.
Pott, C., Krings, M., Kerp, H., 2008. The Carnian (Late Triassic) flora from Lunz in Lower Austria: palaeoecological considerations. Palaeoworld 17, 172–182.
Praehauser-Enzenberg, M., 1970. Beitrag zur Mikroflora der Obertrias von Heiligkreuz (Gadertal, Dolomiten). Festb. Geol. Inst. 300-Jahr. Feier. Univ., Innsbruck, pp. 321–337.
Preto, N., Kustatscher, E., Wignall, P.B., 2010. Triassic climates – State of the art and perspectives. Palaeogeogr. Palaeoclimatol. Palaeoecol. 290, 1–10.
Retallack, G.J., Veevers, J.J., Morante, R., 1996. Global coal gap between Permian-Triassic extinction and Middle Triassic recovery of peat-forming plants. Geol. Soc. Am. Bull. 108, 195–207.
Rigo, M., Joachimski, M.M., 2010. Palaeoecology of late Triassic conodonts: constraints from oxygen isotopes in biogenic apatite. Acta Palaeontol. Pol. 55, 471–478.
Rigo, M., Preto, N., Roghi, G., Tateo, F., Mietto, P., 2007. A rise in the carbonate compensation depth of western Tethys in the Carnian (late Triassic): deep-water evidence for the Carnian Pluvial Event. Palaeogeogr. Palaeoclimatol. Palaeoecol. 246, 188–205.
Roghi, G., 2004. Palynological investigations in the Carnian of the Cave del Predil area (Julian Alps, NE Italy). Rev. Palaeobot. Palynol. 132, 1–35.
Roghi, G., Ragazzi, E., Gianolla, P., 2006. Triassic amber of the Southern Alps (Italy). Palaios 21, 143–154.
Roghi, G., Gianolla, P., Minarelli, L., Pilati, C., Preto, N., 2010. Palynological correlation of Carnian humid pulses throughout western Tethys. Palaeogeogr. Palaeoclimatol. Palaeoecol. 290, 89–106.
Roghi, G., Gianolla, P., Kustatscher, W., Schmidt, A.R., Seyfullah, L.J., 2022. An exceptionally preserved terrestrial record of LIP effects on plants in the Carnian (Upper Triassic) Amber-Bearing section of the Dolomites, Italy. Front. Earth Sci. 10, 900586.
Rostási, Á., Raucsik, B., Varga, A., 2011. Palaeoenvironmental controls on the clay mineralogy of Carnian sections from the Transdanubian Range (Hungary). Palaeogeogr. Palaeoclimatol. Palaeoecol. 300, 101–112.
Ruffell, A., Simms, M.J., Wignall, P.B., 2016. The Carnian humid episode of the late Triassic: a review. Geol. Mag. 153, 271–284.
Ruffell, A., Dal Corso, J., Benton, M., 2018. Triassic extinctions and explosions. Geoscientist 28, 10–15.
Runions, C.J., Owens, J.N., 1996. Pollen scavenging and rain involvement in the pollination mechanism of interior spruce. Can. J. Bot. 74, 115–124.
Schulz, E., 1967. Sporenpaläontologische Untersuchungen rätoliassischer Schichten im Zentralteil des Germanischen Becken. In: Paläontologischen Abhandlungen Abteilung B Paläobotanik, 2, p. 633.
Sciborski, J., Peyrot, D., Lindström, S., Charles, A., Haig, D., Irmis, R.B., 2022. The Enzonalasporites group of Triassic pollen genera and species: New morphological and ultrastructural data, revised taxonomy and paleobiogeographical aspects. Rev. Palaeobot. Palynol. 306, 104744.
Scotese, C.R., 2014. Atlas of Middle & Late Permian and Triassic Paleogeographic Maps, Maps 43–48 from Volume 3 of the PALEOMAP Atlas for ArcGIS (Jurassic and Triassic) and Maps 49–52 from Volume 4 of the PALEOMAP PaleoAtlas for ArcGIS (Late Paleozoic), Mollweide Projection. PALEOMAP Project, Evanston, IL.
Seyfullah, L., Beimforde, C., Dal Corso, J., Perrichot, V., Rikkinen, J., Schmidt, A.R., 2018a. Production and preservation of resins – past and present. Biol. Rev. 93, 1684–1714.
Seyfullah, L., Roghi, G., Schmidt, A.R., 2018b. The Carnian Pluvial Episode and the first global appearance of amber. J. Geol. Soc. Lond. 175, 1012–1018.
Simms, M.J., Ruffell, A.H., 1989. Synchroneity of climatic change in the late. Triassic Geol. 17, 265–268.
Simms, M.J., Ruffell, A.H., 1990. Climatic and biotic change in the late Triassic. J. Geol. Soc. Lond. 147, 321–327.
Simms, M.J., Ruffell, A.H., 2018. The Carnian Pluvial Episode: from discovery, through obscurity, to acceptance. J. Geol. Soc. Lond. 175, 989–992.
Stefani, M., Furin, S., Gianolla, P., 2010. The changing climate framework and depositional dynamics of Triassic carbonate platforms from the dolomites. Palaeogeogr. Palaeoclimatol. Palaeoecol. 290, 43–57.
Sun, Y.D., Wignall, P.B., Joachimski, M.M., Bond, D.P.G., Grasby, S.E., Lai, X.L., Wang, L. N., Zhang, Z.T., Sun, S., 2016. Climate warming, euxinia and carbon isotope perturbations during the Carnian (Triassic) Crisis in South China. Climate warming, euxinia and carbon isotope perturbations during the Carnian (Triassic) Crisis in South China. Earth Planet. Sci. Lett. 444, 88–100.
Tekin, U.K., Krystyn, L., Kürschner, W.M., Sayit, K., Okuyucu, C., Forel, M.-B., 2024. Development of the early Carnian deepening upward sequence of the Huglu Unit within the tectonic slices/blocks of the Mersin M'elange, southern Turkey: Biochronologies, geochemistry of volcaniclastics and palaeogeographic implications. Palaeogeogr. Palaeoclimatol. Palaeoecol. 636, 111964.
Tóth, E., Baranyi, V., Karádi, V., Jin, X., Budai, T., 2024. Ostracod turnover during the Carnian Pluvial Episode (Late Triassic) in the Western Neotethys. Palaeogeogr. Palaeoclimatol. Palaeoecol. 650, 112379.
Trotter, J.A., Williams, I.A., Nicora, A., Mazza, M., Rigo, M., 2015. Long-term cycles of Triassic climate change: a new $\delta^{18}O$ record from conodont apatite. Earth Planet. Sci. Lett. 415, 165–174.
Tyson, R.V., 1995. Sedimentary Organic Matter: Organic Facies and Palynofacies. Springer, Netherlands, Dordrecht, p. 615.
Ueno, K., Kamata, Y., Uno, K., Charoentitirat, T., Charusiri, P., Vilaykham, K., Martini, R., 2018. The Sukhothai Zone (Permian–Triassic island-arc domain of Southeast Asia) in Northern Laos: Insights from Triassic carbonates and foraminifers. Gondwana Res. 61, 88–99.
Ulrichs, M., 1974. Zur Stratigraphie und Ammonitenfauna der Cassianer Schichten von Cassian (Dolomiten/Italien). Schriftenr Erdwiss. Komm. Osterr. Akad. Wiss. 2, 207–222.
Van der Eem, J.G.L.A., 1983. Aspects of Middle and late Triassic Palynology. 6. Palynological investigations in the Ladinian and lower Karnian of the Western Dolomites, Italy. Rev. Palaeobot. Palynol. 39, 189–300.
Végh-Neubrandt, E., 1982. Triassische Megalodontaceae. Akadémia Kiadó, Budapest, p. 526.
Visscher, H., Krystyn, L., 1978. Aspects of Late Triassic palynology. 4. A palynological assembalge from ammonoid-controlled Late Karnian (Tuvalian) sediments of Sicily. Rev. Palaeobot. Palynol. 26, 93–112.
Visscher, H., Van der Zwan, C.J., 1981. Palynology of the Circum-Mediterranean Triassic: phytogeographical and palaeoclimatological implications. Geol. Rundsch. 70, 625–634.
Visscher, H., Van Houte, M., Brugman, W.A., Poort, R.J., 1994. Rejection of a Carnian (Late Triassic) "Pluvial event" in Europe. Rev. Palaeobot. Palynol. 83, 217–226.
Wang, Y.D., Mosbrugger, V., Zhang, H., 2005. Early to Middle Jurassic vegetation and climatic events in the Qaidam Basin, Northwest China. Palaeogeogr. Palaeoclimatol. Palaeoecol. 224, 200–216.
Zapfe, H., 1972. *Cornucardia hornigii* (Bittner) in einer "Dachsteinkalk-Fazies" der Nordalpen. Ann. Naturhist. Mus. Wien 76, 587–604.
Zhang, P., Yang, M., Lu, J., Jiang, Z., Zhou, K., Xu, X., Wang, Y., Wu, L., Chen, H., Zhu, X., Guo, Y., Ye, H., Shao, L., Hilton, J., 2023. Floral response to the Late Triassic Carnian Pluvial episode. Front. Ecol. Evol. 11, 1199121.
Zhang, P., Yang, M., Lu, J., Jiang, Z., Vervoort, P., Zhou, K., Xu, X., Chen, H., Wang, Y., He, Z., Bian, X., Shao, L., Hilton, J., 2024. Four volcanically driven climatic perturbations led to enhanced continental weathering during the late Triassic Carnian Pluvial Episode. Earth Planet. Sci. Lett. 626, 118517.